Bulletin 15

New Mexico Museum of Natural History and Science

A Division of the

OFFICE OF CULTURAL AFFAIRS

# A New Skull of *Parasaurolophus* (Dinosauria: Hadrosauridae) from the Kirtland Formation of New Mexico and a Revision of the Genus

by

Robert M. Sullivan[1] and Thomas E. Williamson[2]

[1]The State Museum of Pennsylvania
[2]New Mexico Museum of Natural History and Science

Published with the support of the
United States Bureau of Land Management and
The State Museum of Pennsylvania, Pennsylvania Historical and Museum
Commission, Harrisburg

ALBUQUERQUE, 1999

**Cover illustration:**
**Short and long-crested species of *Parasaurolophus* in a hypothetical co-existence, by Richard Penney**



*Original Printing*

Published by Authority of the State of New Mexico

Available from the New Mexico Museum of Natural History and Science, 1801 Mountain Road NW, Albuquerque, NM 87104
Telephone (505) 841-2800; Fax (505) 841-2866

# A New Skull of *Parasaurolophus* (Dinosauria: Hadrosauridae) from the Kirtland Formation of New Mexico and a Revision of the Genus

*by Robert M. Sullivan and Thomas E. Williamson*

CONTENTS

*"I have learned, after an experience of over fifty years in the fossil fields of North America, that the only way to secure dinosaur skeletons, or even skulls, is to go carefully over every square foot of exposed surface, the mind wholly occupied with this one thought, and the eyes seeing nothing but the object of the hunt. The most valuable specimen may be easily passed over, especially if the mind dwells on something else."*

-Charles H. Sternberg, 1932, p. 221.

(recounting his collecting activities in the San Juan Basin, New Mexico, from Chapter 16, "Lost in the Desert," in *Hunting Dinosaurs in the Bad Lands of the Red Deer River, Alberta, Canada*, revised, 2nd edition)

# A NEW SKULL OF *PARASAUROLOPHUS* (DINOSAURIA: HADROSAURIDAE) FROM THE KIRTLAND FORMATION OF NEW MEXICO AND A REVISION OF THE GENUS

ROBERT M. SULLIVAN[1] and THOMAS E. WILLIAMSON[2]

[1]Section of Paleontology and Geology, The State Museum of Pennsylvania, Third and North Streets, Harrisburg, PA 17108-1026; [2]New Mexico Museum of Natural History and Science, 1801 Mountain Road, NW, Albuquerque, NM 87104-1375

**ABSTRACT**: A new skull and left lower jaw of the rare lambeosaurine hadrosaur *Parasaurolophus tubicen* Wiman, 1931, was recently discovered and recovered from the De-na-zin Member of the Kirtland Formation, Bisti/De-na-zin Wilderness, San Juan County, New Mexico. Although incomplete, the specimen (NMMNH P-25100) compares readily to the holotype (PMU.R1250) and ranks as the second most complete skull of the genus and the second definitive specimen of this species. Excellent preservation allows for the discrimination of sutures that define the bones of the upper skull and narial crest regions for the first time and thus settles long-standing debate concerning interpretation of the cranial sutural pattern.

Computer tomographic analysis of the internal structure of the narial crest of NMMNH P-25100 reveals a complex network of tubes heretofore unknown in *Parasaurolophus*. The tubes of the crest consist of: 1) a dorsal pair that extend from the external naris to the tip of the crest where they terminate in paired chambers; 2) two pairs that extend from the external naris to the wall of the terminal chamber, U-bend and return anteriorly, coalescing into a single pair of tubes, and coalescing with a pair of inner tubes (the lateral diverticulae); and 3) an innermost pair (the lateral diverticulae) that extend from the anterior part of the skull below the two pairs of tubes, and posteriorly form a tight U-bend and return ventrally to coalesce with the ventralmost tubes and descend into the choana.

A revision of the genus suggests that the three named species are valid and that *Parasaurolophus cyrtocristatus* is the sister-taxon to *P. walkeri* and *P. tubicen*. Moreover, *P. cyrtocristatus* is interpreted as a structural ancestor to the long-crested forms represented by *P. walkeri* and *P. tubicen*. The complex narial crest of *P. tubicen* is considered the most derived of the three taxa, and *Parasaurolophus* is considered the most derived lambeosaurine.

Biostratigraphic distribution of the three species of *Parasaurolophus* is equivocal due to the uncertainty of the type locality of *P. cyrtocristatus* and the absolute age of the lower part of the Kaiparowits Formation which yielded two additional specimens of *P. cyrtocristatus*.

One of us (RMS) favors the hypothesis that the auxilliary function of the crest of *Parasaurolophus* evolved for visual display for species, not gender recognition, while the other author (TEW) suggests that the crest served as both a visual and an acoustic display structure, especially for intraspecific recognition.

## INTRODUCTION

Perhaps the most beloved, and the most profusely illustrated, hadrosaurid dinosaur is *Parasaurolophus*. Yet, ironically, this dinosaur is known from only a few specimens (Fig. 1). Until very recently, only four specimens had been recovered: two of the long-crested variety and two short-crested ones. The narial crest, a term coined by Ostrom (1961a) to denote "true narial crests" of lambeosaurines versus "pseudonarial crests" as exemplified by *Prosaurolophus*, *Saurolophus*, and *Brachylophosaurus*, is used here to denote a type of skull crest composed largely of nasal passages that serve as primary conduits between the external nares and the internal trachea. The distinctive, unusual elongated narial crest of *Parasaurolophus*, especially that of the long-crested morph, has been the subject of much speculation and interpretation (see below).

*Parasaurolophus* is known only from western North America (Fig. 2). The first specimen of *Parasaurolophus* was discovered by L. W. Dippell, and collected by Levi Sternberg, in 1920 in the Dinosaur Park Formation (formerly Oldman Formation, in part, and equals Belly River beds, in part) of Alberta (Eberth and Hamblin, 1993). It consists of a complete long-crested skull and partially complete postcranial skeleton that was described and named *Parasaurolophus walkeri* (ROM 768) by Parks (1922). A second long-crested specimen, consisting of a partial skull, was discovered and collected by veteran dinosaur hunter Charles H. Sternberg in 1921 from the Upper Cretaceous Kirtland Formation (?De-na-zin Member, see below) of New Mexico (Fig. 3), while under the employ of Swedish paleontologist Carl Wiman. This specimen (PMU.R1250) was described and given the name *Parasaurolophus tubicen* by Wiman (1931). A third specimen (FMNH P27393), this time a short-crested skull and partial postcranial skeleton, putatively from the Fruitland Formation (Ostrom, 1961b; 1963, see discussion below) of northwestern New Mexico (Fig. 3), was also discovered and collected by C. H. Sternberg in 1923. It was described years later by Ostrom (1961b, 1963) and given the name *Parasaurolophus cyrtocristatus*. In 1971, Jim Jensen discovered a partial skull and narial crest in the Upper Cretaceous Kaiparowits Formation of Utah. It was later described by Weishampel and Jensen (1979) as *Parasaurolophus* sp. We have since determined that this specimen (BYU 2467) belongs to the short-crested species, *P. cyrtocristatus* (see below). Recently, a third short-crested specimen (*P. cyrtocristatus*) was recovered from the lower part of the Kaiparowits Formation of Utah by J. Howard Hutchison in 1995 and will be described by him elsewhere.

On August 17, 1995, one author (RMS) found a nearly complete skull of long-crested *Parasaurolophus tubicen* in the Upper Cretaceous

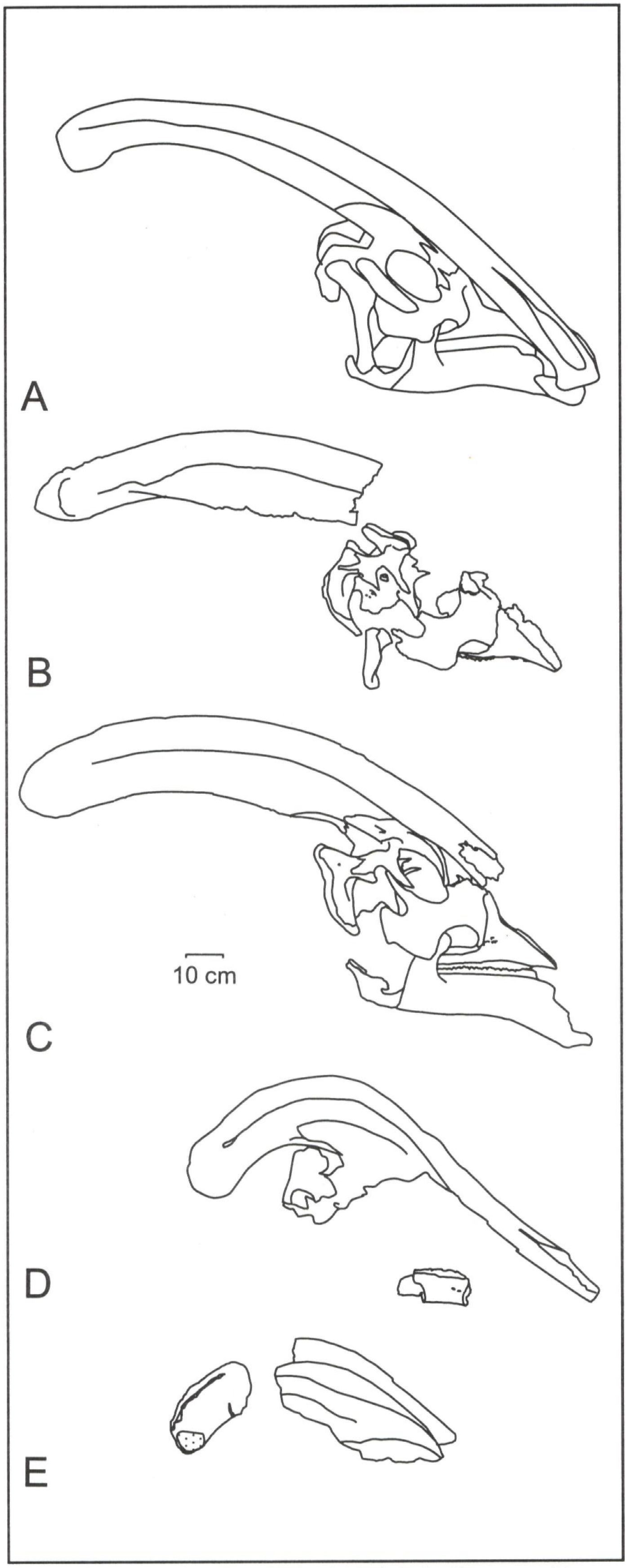


**Figure 1**. Specimens of *Parasaurolophus* that include significant parts of the crest that are discussed in this paper. A, ROM 768, holotype of *P. walkeri*; B, PMU.R1250, holotype of *P. tubicen*; C, NMMNH P-25100, *P. tubicen*; D, FMNH P27393, holotype of *P. cyrtocristatus*; and E, BYU 2467, *P. cyrtocristatus*.

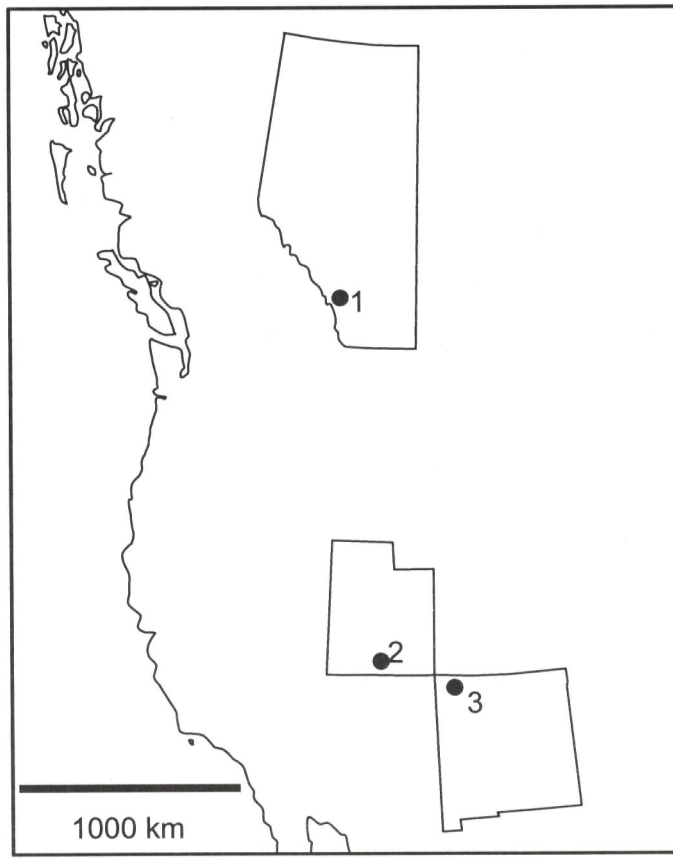


**Figure 2**. Map of western North America showing localities where *Parasaurolophus* specimens have been recovered. 1, Dinosaur Park Formation, Alberta, Canada; 2, Kaiparowits Formation, Utah; 3, Fruitland and/or Kirtland Formation, New Mexico.

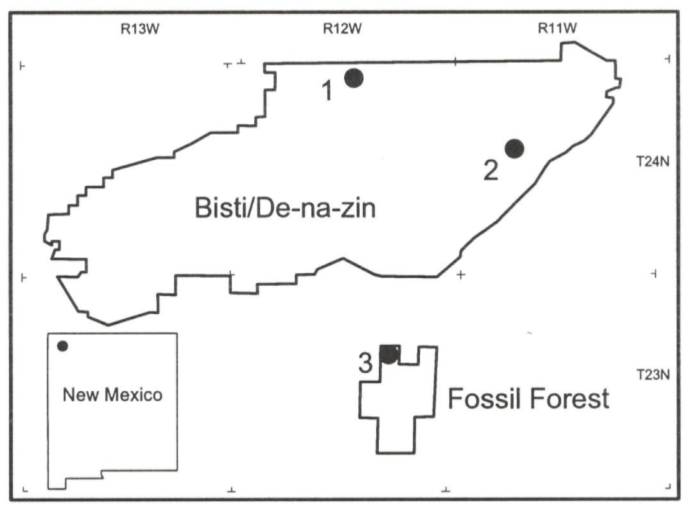


**Figure 3**. Locality of new *Parasaurolophus tubicen* specimen (NMMNH P-25100; locality L-3347) and other specimens of *Parasaurolophus* in relation to the Bisti/De-na-zin Wilderness Area and Fossil Forest Natural Research Area, San Juan Basin, New Mexico. 1, locality L-3347; 2, locality for PMU.R1250, holotype of *P. tubicen* (after Hunt et al., 1992); 3, probable locality for FMNH P27393, holotype of *P. cyrtocristatus*.

Kirtland Formation (De-na-zin Member) of northwestern New Mexico (Fig. 3). The well-preserved specimen (NMMNH P-25100), which includes a nearly complete crest, posterior skull bones, left maxilla, jugal and mandible, is the second most complete skull of this genus and the most complete one of this species known. The specimen was briefly reported on by us (Williamson and Sullivan, 1996), and its internal crest structure was the subject of a separate report (Sullivan and Williamson, 1996).

Here, we describe the new specimen in detail (both internal and external aspects), reassess the previous specimens and revise the genus *Parasaurolophus*, review the biostratigraphic distribution and phylogenetic systematics of *Parasaurolophus*, and revisit the issue of the functional morphology of the narial crest in the light of new data.

## INSTITUTIONAL ABBREVIATIONS

BYU-- Brigham Young University, Provo
FMNH-- Field Museum of Natural History, Chicago
KU-- University of Kansas, Lawrence
MNA-- Museum of Northern Arizona, Flagstaff
NMMNH-- New Mexico Museum of Natural History and Science, Albuquerque
PMU-- Paleontologiska Museet, Uppsala
ROM-- Royal Ontario Museum, Toronto
UCMP-- University of California, Museum of Paleontology, Berkeley
USNM-- United States National Museum, Washington, D. C.

## PART 1. SYSTEMATIC PALEONTOLOGY

### DINOSAURIA Owen, 1842
### ORNITHISCHIA Seeley, 1887
### HADROSAURIDAE Cope, 1869
### LAMBEOSAURINAE Parks, 1923
### *PARASAUROLOPHUS* Parks, 1922

**Type Species**-- *Parasaurolophus walkeri* Parks, 1922, p. 5.

**Revised diagnosis**-- A lambeosaurine hadrosaur differing from all other hadrosaurs in having a short, or long, tubular, slightly curved, narial crest composed largely of the premaxillae$_1$. Prefrontals lapping on to the ventral lateral surface of premaxillae$_1$ where the skull roof and narial crest meet. Frontals arising from the posterior base of the narial crest and extending posteriorly, where they articulate with the nasals at a point before the farthest extent of the squamosals. Nasals confined to the ventral margin of the anterior part of the narial crest, extending a short distance beyond the posterior-most extent of the frontals. Premaxillae$_2$ forming the lower border of external naris, extending posteriorly, each flanked by the lateral groove below (separating the premaxilla$_2$ from the maxilla), and terminating just beyond the dorsal apex of the maxilla.

**Discussion**-- In his paper, Parks (1922) described, but did not diagnose, *Parasaurolophus walkeri*. His rationale for establishing this taxon was based principally on two features: a "low-set and heavy body" coupled with a "very remarkable type of crest" (Parks 1922:5). Twenty years later, in their classic monograph, Lull and Wright (1942) provided the first characterization of the genus based on the then known specimens: the holotypes of *P. walkeri* and *P. tubicen*, the latter having been described by Wiman (1931). Since Lull and Wright's diagnosis of the genus *Parasaurolophus*, four additional specimens have come to light, three of which are short-crested and have been referred to *Parasaurolophus*, thus mandating a reassessment of the characters that diagnose this genus.

A few generic characters, listed by Lull and Wright (1942), are not considered by us as diagnostic, because they are either size-related, or variable, and are seen, to some extent, in other hadrosaurids. These include: large external (anterior) nares (which may be exaggerated in ROM 768 owing to crushing and distortion), infratemporal fossa narrow for its entire length (four times long as wide), proportions similar to those of *Edmontosaurus*; long paroccipital process (not that much longer than in other hadrosaurs, extends halfway down the length of the quadrate); quadratojugal separates jugal from the quadrate (a number of hadrosaurs have a well-developed quadratojugal with only the jugal and quadrate directly in contact dorsally; verification of this condition in the two specimens of *P. tubicen* is not possible, see below). The edentulous portions of the lower jaws are probably the shortest for *Parasaurolophus*. They are shorter in all lambeosaurines than in hadrosaurines, but this difference is difficult to quantify. The sigmoidal lower margin of the mandible is a feature that is also present in other lambeosaurines and is not unique to *Parasaurolophus*. The "lower branch of the premaxilla" (premaxilla$_1$) is approximately the same length and position as in a number of hadrosaurines, and presumably represents the primitive condition. However, in many of the helmeted lambeosaurines, the premaxilla$_1$ extends posteriorly and is incorporated into the crest of the dinosaur (a derived feature). Other characters of dubious importance include: large scapula; short and stout forelimbs; and slope of spines of the 19th and 20th dorsal vertebrae unique. These characters are difficult to assess, not only due to their ambiguity, but also because too few postcranial remains of *Parasaurolophus* are known. Thus, the consistency of these features cannot be demonstrated. Moreover, differences among the two species that are known by postcranial material (*P. walkeri* and *P. cyrtocristatus*) are variable. However, Brett-Surman (1975, 1989), in his studies of hadrosaur postcrania, did suggest some characters as being diagnostic of *Parasaurolophus*. These include: unusually large and robust antitrochanter (separates *Parasaurolophus* from less derived hadrosaur genera); length/width ratio of the postacetabular portion of the ilium is shorter and higher compared to derived hadrosaurines; tall prepubic process (shared with *Tsintaosaurus* and *Bactrosaurus*); and reduced tarsus, lacking calcaneum, with astragalus in the form of an isoceles triangle (type 2 tarsus), which is only known in *Parasaurolophus cyrtocristatus* (Brett-Surman, 1989).

Other generic features of *Parasaurolophus* noted by Brett-Surman (1989), compared to other hadrosaurids, include: 1) relatively short and wide scapular blade; 2) more robust humerus (in *P. cyrtocristatus*); 3) radius shorter than the humerus (compared to other lambeosaurines, but similar to ratios seen in other hadrosaurines); 4) relatively thicker ulnae; 5) robust carpals; 6) robust ilium (thicker and wider) with a pronounced preacetabular process deflected ventrally; 7) pubis relatively shorter and wider compared to others (a feature shared with *Bactrosaurus*); 8) robust ischium with prominent posteriorly projecting "lip" on iliac peduncle (shared with *Hypacrosaurus*); 9) tibia with greatly expanded distal end; and 10) calcaneum lost, but this may be an artifact of preservation or failure to ossify with the fibula expanding to compensate.

A majority of these characters, based primarily on the holotype postcranial skeleton of *P. cyrtocristatus,* shares "robustness," which is ambiguous and may reflect relative size and maturity of the specimen rather than offering anything of taxonomic significance. The broad range of shared features among other hadrosaurs, especially from the outgroup (hadrosaurines), suggests that they are primitive characteristics and therefore are not phylogenetically significant (see discussion below). Suffice it to say that because of the lack of postcranial comparative material many of these features are dubious for taxonomic purposes.

However, a number of skull characters cited by Lull and Wright (1942) have taxonomic utility and are valid features useful for diagnosing the genus as they are verifiable among the three named species. The narial crest, both the short and long-crested varieties, certainly sets *Parasaurolophus* apart from all other lambeosaurine hadrosaurs. The narial crest is curved, or arched, in both the long-crested and short-crested forms, although the curve is more pronounced in the latter. Clearly, any diagnosis of *Parasaurolophus* is dependent on an unambiguous interpretation of the bones of the skull and the narial crest. There have been numerous interpretations over the years, which are worth summarizing here.

The bones that compose the narial crest of the skull of *Parasaurolophus*, specifically the holotype of *P. walkeri* (ROM 768), have been re-interpreted in numerous technical publications (most notably Parks, 1922; Wiman, 1931, Lull and Wright, 1942; Russell, 1946; Ostrom, 1961a, b, 1963; Hopson, 1975; Weishampel and


**Figure 4**. *Parasaurolophus walkeri* (ROM 768, holotype) close-up left lateral view of skull. The circular object within the orbit is the head of a metal spike.

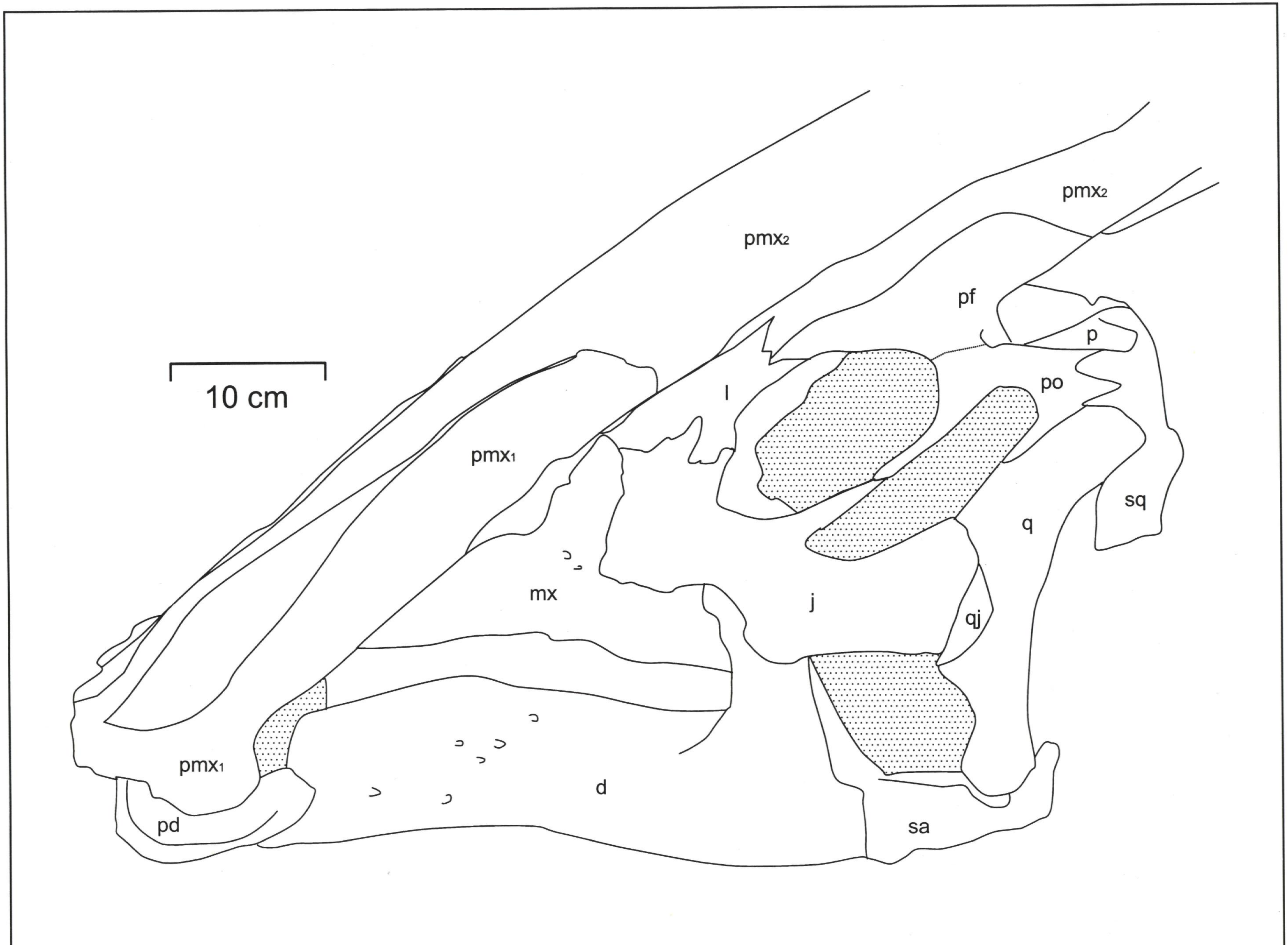


**Figure 5**. *Parasaurolophus walkeri* (ROM 768, holotype) interpretive line drawing showing revised suture pattern. See Appendix 1 for osteological abbreviations.

Jensen,1979; Weishampel, 1981a, b; and Weishampel and Horner, 1990). Parks (1922) described and illustrated the skull and narial crest of ROM 768. In his interpretation, the undifferentiated premaxillae were restricted to the anteriormost part of the snout lying in front of the anterior projection of each maxilla. Although no suture separating the premaxillae from the nasals was detectable, he interpreted the nasals as comprising the dorsal part of the narial crest, extending from the anterior part just behind the external nares to the tip of the crest. He believed that the "deeply incised suture" (i.e., the lateral groove) separated the superior "nasals" and the frontals, and maxillae below. Parks (1922) interpreted the left side of the skull of ROM 768 as having the frontal extending from the tip of the crest anteriorly to meet (articulate) with the lacrimal, prefrontal and jugal. This region, which was later the focus of a short paper by Russell (1946), was interpreted by Parks (1922) as having the prefrontal reduced to a small triangular element surrounded by the lacrimal anteriorly and anterodorsally, the frontal posteriorly and posterodorsally, and by the jugal ventrally. We now know that the "frontal" is actually the lacrimal, bounded by the maxilla below (see below). The "prefrontal" is actually part of the lacrimal, the "suture" dividing the "maxilla" and "lacrimal" does not exist and that the latter is part of the maxilla. The other skull elements were correctly presented by Parks.

Wiman (1931) revised Parks' interpretation of the bones of the narial crest and upper part of the skull. He recognized that the premaxillae composed the dorsal component of the crest, and the nasals the ventral component. The nasals met the frontals near the base of the crest, which in turn joined with the prefrontals and lacrimals on either side. Wiman's (1931) illustration of the specimen lacked sutures between these respective elements.

Lull and Wright (1942) presented another, more correct interpretation of these bones. First, they observed that the premaxillae were divisible into two components. The premaxilla$_1$, which composes the greatest part of the narial crest, and the premaxilla$_2$, form the inferior border between the external naris and the maxilla. However, the premaxilla$_1$ was interpreted as being restricted to the dorsal component of the narial crest, with both the frontals (anteriorly) and nasals (posteriorly) forming the ventral part of the crest.

Russell (1946) improved on the interpretation of Lull and Wright (1942), recognizing that the premaxilla$_2$ made up both the ventral and dorsal components of the crest and that these bones contacted the nasals and prefrontals on either side above the orbit. However, Russell was unable to delineate the lacrimal, prefrontal, nasal, frontal and premaxilla$_2$ within the orbital region.

Ostrom's (1961a, b and 1963) interpretation departed from the previous ones in that he was able to circumscribe the extent of the prefrontal, lacrimal and nasal. The prefrontal is a sub-rectangular bone lying anteriorly and participating posteroventrally with the orbit. Anteroventrally, is a small triangular lacrimal with its posterior margin participating in the anterior orbital border. The nasal occupies a region above the contact of the prefrontal/postorbital. This interpretation was repeated by Hopson (1975).

A subsequent interpretation presented by Weishampel and Jensen (1979), and later repeated by Weishampel (1981a, b), was even more accurate. These two studies recognized that the prefrontal arises over the orbit and extends posteriorly. However, the nature and extent of the prefrontal contact with the lacrimal anteriorly was not delineated. Concomitantly, the nature and extent of the prefrontal posteriorly was not established. Weishampel interpreted the nasal rising from above the prefrontal and extending posteriorly adjacent to the lateral groove part way up the narial crest and bounded ventrally by the premaxilla$_1$ just above the postorbital-squamosal contact on the skull roof. This interpretation was slightly modified by Weishampel and Horner (1990), who correctly delineated the lacrimal/prefrontal contact, but retained the previous interpretation of the prefrontal/nasal juxtaposition. We now know that this interpretation is incorrect and that the prefrontals extend posteriorly along the lateral sides of the narial crest, below the lateral groove, and taper to a point in a near vertical plane just short of the posterior-most extent of the squamosals. Below the posterior extension of the prefrontals lie the frontals and nasals, the latter articulating with the frontals anteriorly, just before the posterior-most extent of the prefrontals (see description of NMMNH P-25100, below).

It is interesting to note that Wilfarth (1949), in his illustration of *P. tubicen*, had correctly interpreted the position of the lacrimal and prefrontal with respect to the orbit, but not the posterior extent of the latter element.

### *PARASAUROLOPHUS WALKERI* Parks, 1922
### Figures 1A, 4, 5

**Holotype**-- ROM 768, complete skull and narial crest (Fig. 1A, 4, 5), with incomplete postcranial skeleton.

**Revised diagnosis**-- A long-crested *Parasaurolophus* differing from *P. tubicen* in having a narial crest consisting of two dorsal tubes that extend posteriorly, U-bend at the apex of the narial crest and return along the ventral margin where they coalesce (internally) with the lateral diverticula. Dorsal and ventral tracts separated by a lateral groove on each side of the narial crest. Differs from *P. cyrtocristatus* in having an elongated narial crest, more than twice the length.

**Redescription**-- The skull of ROM 768 has been described by Parks (1922) and redescribed by Lull and Wright (1942). Our study of the specimen has little to add to these previous descriptions; however, we note some features of specific regions of the skull not reported in previous studies.

There is a section on the anteroventral side of the crest that may represent the frontal. At the time of our initial examination, the area was covered with plaster and painted, making it nearly impossible to determine, with any level of confidence, the configuration of this paired element. Fortunately, the left side of the skull has since been cleaned and restored and is illustrated here for the first time (Figs. 4, 5). It is possible that the narial crest has been deformed so that the left frontal has been relocated to the right side. The posteriormost extension of the frontal is visible on the left side. Therefore, we suggest that both frontals have been displaced and are now visible on the right side.

On the whole, the nasal sutures are not clearly delineated, but there is evidence of a suture rising above the posteriormost extent of the parietal. Anteriorly, the suture disappears into a region that is crushed, poorly preserved, and unprepared. There is no evidence of a foramen in this region as seen in NMMNH P-25100 (see below).

The dorsal surfaces of the premaxillae$_2$ (narial crest) are smooth, lacking the anastomosing furrows seen in both NMMNH P-25100 and PMU.R1250 (see below). It appears that the dorsal segment of the crest in ROM 768 is more inflated, rather than laterally compressed (however, this may be a result of crushing in the specimens of *P. tubicen*). The narial crest of ROM 768 is longer and less deep compared to NMMNH P-25100 and PMU.R1250 (see measurements in Appendix 2). The tip of the crest is deformed on both sides, obscuring any structure that could be utilized for diagnostic purposes. The surface of the crest is relatively smooth both above and below the lateral groove.

We found no major differences between the left jugal of ROM 768 and NMMNH P-25100. However, the maxillary foramina clustered toward the anterior end of the left jugal present in NMMNH P-25100 and PMU.R1250 (see below) are not visible.

**Discussion**-- Because this comparative study is concerned solely with the skulls and lower jaws of *Parasaurolophus*, our comments are limited to these skeletal elements. ROM 768 has served as the standard for the genus *Parasaurolophus* since its discovery and description by Parks (1922). Unfortunately, the skull has not been fully prepared, particularly its right side. Consequently, the arrangement of sutures of the skull have been quite problematic, resulting in numerous published interpretations (as noted above). In addition, because the skull is articulated, it is not possible to view adequately the bones of the palate and basicranium. The holotype is the only known specimen of this species.

### *PARASAUROLOPHUS TUBICEN* Wiman, 1931
### Figures 1B, C, 6-21

**Holotype**-- PMU.R1250, incomplete skull and narial crest (Figs. 1B, 6-11).

**Revised diagnosis**-- A long-crested *Parasaurolophus* that differs from *P. walkeri* and the short-crested *P. cyrtocristatus* in having an internally more complex narial crest consisting of a pair of dorsal tubes that extend from the external naris and terminate posteriorly, forming the apex of the narial crest below two pairs of tubes that extend from behind the external narial openings (and presumably are contiguous with them) forming a U-bend posteriorly where they coalesce into a single pair of ventral tubes and return anteriorly, forming the ventral margin of the narial crest where they rise slightly above the nasal and frontal region and fuse with the ventral tubes of the lateral diverticulae above before entering the choana; lateral divertculae are paired, arise anteriorly (presumably communicate with the external nares), extend posteriorly, forming a tight U-bend and return ventrally above the ventral tubes and coalesce with the ventral tubes anteriorly before entering the choana. Dorsal and dorsolateral exterior surface of the narial crest bearing anastomosing furrows. Differs from *P. cyrtocristatus* in having a long narial crest.

**Redescription**-- Wiman (1931) described this skull in detail. Here, we take the opportunity to reiterate some observations made by him and make comparisons to the new specimen described below.

The incomplete narial crest of the holotype of *Parasaurolophus tubicen* (PMU.R1250; Fig. 6) is remarkably similar to the corresponding section of the narial crest of NMMNH P-25100. The narial crest section of the holotype measures approximately 93 cm along the lateral groove from the apex of the crest forward. The lateral groove extends for nearly the entire length to approximately 12 cm from the apex.

The right side of the crest is distorted in places, especially in a region approximately 30 cm from the apex of the narial crest, where the dorsal surface is folded over the lateral groove. Anastomosing furrows are prominent on the dorsal and lateral surfaces of the dorsal component (as in NMMNH P-25100, see description below) and extend dorsoposteriorly from the lateral groove. The distal ends of the frontals are preserved proximally along the ventral margin of the narial crest. The frontals bear fine striations that are also directed dorsoposteriorly (these are distinct from the anastomosing furrows of the dorsal component). The exterior surface of the ventral component of the narial crest section lacks anastomosing furrows. The anterior part of the narial crest is broken, revealing the crest in cross-section (Fig. 7). Anteriorly, chambers, infilled with matrix, and restored areas (black plaster) are evident. The distal end is crushed, presumably where the tubes make their U-bends. The distal-most tip is unrushed but presumably laterally compressed to some extent.

The left side of the preserved crest is slightly distorted. The ventral component is folded up against the lateral groove anteriorly. As on the right side, anastomosing furrows are present on the dorsal component of the crest. Distally, a large region is eroded to form a "window," exposing a large pair of the lateral tube series of the dorsal component. A prominent groove arises approximately 54 cm from the apex of the crest and extends posteriorly. A fine ventral groove is visible posteriorly along the ventral surface. It arises approximately 7 cm from the tip of the crest, reaching posteriorly for 40 cm, where it ends due to breakage. A dorsal groove is less prominent, obscured by crushing and distortion for nearly the entire length of the crest section. The broken end shows (Fig. 7) a similar arrangement of tubes in cross-section as described below for NMMNH P-25100.

The suture between the frontals and the parietals (Figs. 8A, B and 9A, B) is high on the skull roof, lying below the ventral part of the narial crest. The parietal rises a short distance above the back of the narial crest in the region of the ventral crest base. Here it meets the frontal, and the parietal extends from the inflexion point (measured 3.0 cm) to the contact with the frontal.

The lateral contact between the right parietal/squamosal (Figs. 8B, C and 9B, C) is not distinct. The surface in this region is marked by a rough texture dorsally, but is largely obscured by plaster and breakage. In posterior view, the parietal is visible at the apex, flanked ventrally by the exoccipital. The supraoccipital is exposed ventrally below the point where it emerges between the squamosals medially. The medial part is distinguished by a rugose texture. The supraoccipital section is surrounded by a depression, or cavity, on the right, left, and dorsal sides. It contacts the supraoccipital (Wiman's "opisitcum") immediately on both sides. The height of the parietal as measured to the base of the supraoccipital (posterior view) is 11.18 cm. The parietal within the supratemporal region is marked by a very thin, high sagittal crest that is inflected dorsally and posterolaterally. Along the ventral margin there is a prominent ridge that presumably marks the contact with the exoccipital/opistotic/laterosphenoid complex.

The right postorbital (Figs. 8A, B and 9A, B) closely corresponds to that in the new specimen, except that the posterior projecting process that overlaps onto the squamosal is longer and narrower. It is reminiscent of the sigmoidal suture exhibited in NMMNH P-25100. The left postorbital is obscured by plaster. Wiman's interpretation of this region is inconsistent with his illustration, where he indicated a broad posterior postorbital process overlapping the squamosal. Foramina near the postorbital/nasal contact are the same as in NMMNH P-25100. The anteroventral projecting process of the postorbital measures 7.9 cm and conforms to NMMNH P-25100.

The positions of the cranial foramina (Figs. 8A, B and 9A, B) roughly correspond to those seen in NMMNH P-25100. Some minor differences include the spacing between the foramina for cranial nerves IX, XI and XII. The distance between cranial nerve foramina XI and XII is closer in the holotype of *P. tubicen*. The exit of the dorsal (anterior) branch of the trigeminal nerve ($V_1$) is obscured by plaster. The large, anterior-most opening may represent the foramen for the cranial nerve II. A small process of the basisphenoid projects ventroposteriorly over the foramen for the internal carotid artery.

As in NMMNH P-25100, in lateral view, many of the bones that compose the basicranium are fused, obliterating sutural contacts. On the right side, there is a line between the exoccipital process and the basioccipital that may correspond to a suture and/or fracture. This region is not clear on the left side of the basicranium.

Anteriorly, there is an irregular ridge that may mark the contact of the basisphenoid and parasphenoid. Dorsally, there is a juncture of the laterosphenoid, orbitosphenoid and presphenoid.

The basioccipital (Figs. 8D,E and 9D,E) consists of a prominent medial condyle marked by a medial groove; below lie two (paired) knobs that we consider part of the basioccipital as identified by Wiman (1931) and contrary to Ostrom (1961, fig. 11, p. 59). Ventrally, the basioccipital contacts the basisphenoid, however, the sutures between these bones are not evident. The surface of the lower portion of the basioccipital is extremely rugose.

The basisphenoid (Figs. 8E-9E) is distinguished by a rugosity on the dorsal end where it joins the basioccipital. A crack, which presumably marks the suture between the two bones, is evident on the lateral sides as well as on the ventral surface. No contact between the basisphenoid and presphenoid is discernible, as they are indistinguishably fused. The wings of the basisphenoid are separated by a deep sulcus that narrows anteriorly where they merge with the single parasphenoid process.

The right maxilla of the holotype (Figs. 10-11) is very similar to the left maxilla of NMMNH P-25100 in size and form, so its measurements are consistent with those of the new specimen (see Appendix 2). Anteriorly, the contact surface with the right premaxilla$_2$ is wide, approximately 6 cm at its maximum width. The maxilla and the


**Figure 6**. *Parasaurolophus tubicen* (PMU.R1250, holotype). Posterior part of the narial crest in (A) right lateral view and (B) left lateral view.

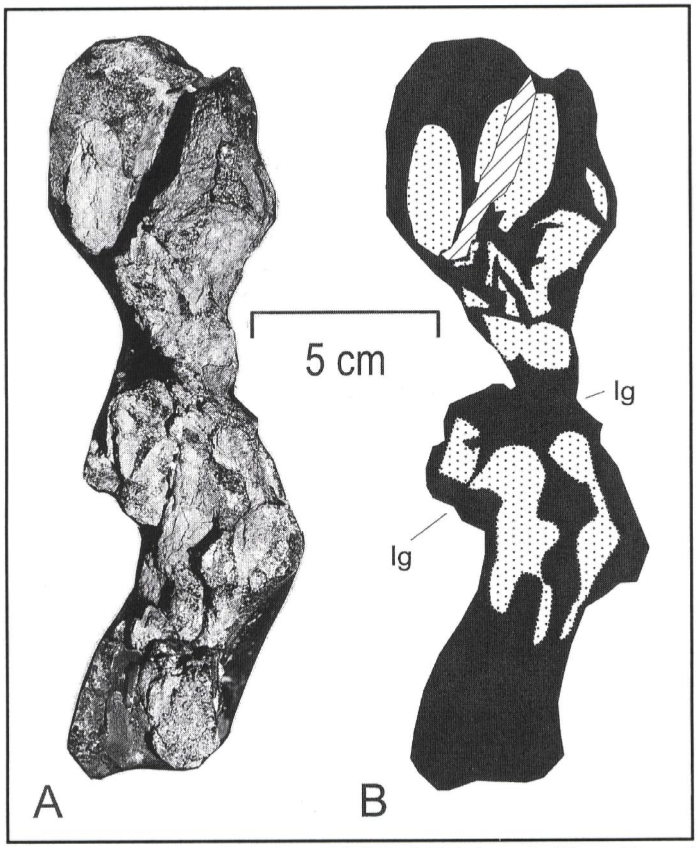


**Figure 7**. *Parasaurolophus tubicen* (PMU.R1250, holotype). View of base of crest at natural break (A) and interpretive line drawing (B). See Appendix 1 for osteological abbreviation.

articulated jugal are fractured on the upper lateral surface, which is depressed and filled with matrix. The lacrimal/jugal contact is prominent. The maxillary foramen is obscured by matrix.

The anteriomedial part of the right jugal (Figs. 10A-11A) is crushed along with the corresponding underlying part of the maxilla. There is breakage at the anteroventralmost part of the jugal. The jugal/lacrimal contact is strong as in NMMNH P-25100. The jugal lacks the small depression along the ventral margin that is present in NMMNH P-25100. The distal parts of both the quadratojugal and postorbital extension are missing (broken).

The palatine is incomplete (Figs. 10-11), lacking most of the posterior part. The preserved posterior part is highly fractured and infilled with matrix in most places. The palatine is best preserved along the maxilla/palatine contact, especially along the dorsalmost region. Anteriorly, the dorsalmost contact is marked by a prominent sinuous suture, which becomes less distinct ventrally. The contact with the ectopterygoid is broad, measuring 3.3 cm at its widest point and 8.7 cm in length (incomplete). This element corresponds to the "GPt" in Wiman (1931; plate 1, fig.2).

**Discussion**-- The holotype of *P. tubicen* departs from *P. walkeri* in: 1) having a greater number of narial crest tubes and a more complex arrangement of these tubes; and 2) presence of anastomosing furrows on the dorsal component of the narial crest (above the lateral groove). It is nearly identical in every respect to the new referred specimen described below, suggesting that there are two valid species of the long-crested morph.

**Newly Referred Material**-- NMMNH P-25100, skull and lower jaw consisting of the left jugal, left maxilla, skull roof consisting of lacrimals, prefrontals, frontals, nasals, and nearly complete narial crest (premaxillae$_2$), basicranium, left dentary, left angular, left surangular, and left articular (Figs. 12-21).

**Locality**-- NMMNH Loc. 3347, tributary of Hunter Wash, San Juan Basin, New Mexico.

**Horizon**-- Kirtland Formation (De-na-zin Member), approximately 9.3m (30 feet) below the base of the lower conglomerate (contact between the upper De-na-zin Member and lower Naashoibito Member and 13.1m (41 feet) below the base of upper conglomerate contact of the upper Naashoibito Member and the lower part of the Ojo Alamo Sandstone).

**Age**-- Late Cretaceous (late Campanian).

**Collectors** (in alphabetical order)-- Ray Geiser, Pete Reser, Warren Slade, Robert M. Sullivan, Michael Tipping, and Thomas E. Williamson, August 1995.

**Description of Skull and Mandibular Elements**-- The following osteological description of the skull is based on cranial elements from the right side of the specimen with the exception of the jugal and maxilla that are from the left side. The description of the mandibular elements is based on the remains of the left mandible.

**Skull and Narial Crest Elements**

**Premaxilla$_1$**-- Not recovered.

**Premaxilla$_2$**--The premaxillae are here represented by most of both paired premaxillae$_2$. The premaxillae$_2$ compose the largest bone mass, covering the greatest surface area, that of almost the entire narial crest (Fig. 12). Together with minor contributions of the nasals, frontals and prefrontals (see description above), these elements form the distinct narial crest of *Parasaurolophus*. The internal morphology of the narial crest is described in detail below. The lateral sides of the premaxilla$_2$ are crushed and slightly imbricated and wrinkled in part. The lateral walls formed by the premaxillae$_2$ are very thin, less than a few millimeters thick in places. The surface of the upper portion of the premaxilla$_2$ (above the lateral groove) is characterized in part by a broken network of anastomosing furrows (Fig. 13). The surface of the lower part of the premaxilla$_2$ (below the lateral groove) is relatively smooth. Ventrally, the premaxillae$_2$ contact the dorsal borders of the lacrimals, prefrontals, nasals and frontals. The premaxillae$_2$ do not contact the parietals. The apex formed by the premaxillae$_2$ (narial crest) is parabolic, not U-shaped. The premaxillae$_2$ are compressed laterally; some of this compression is due to crushing. On the right side, the anterior margin of premaxilla$_2$ is apparently the suture that contacts premaxilla$_1$.

**Maxilla (including the maxillary tooth battery)**-- The left maxilla is large and triangular (Figs. 14A, B, 15). In lateral (labial) view, the portion of the maxilla between the premaxilla$_1$ and the jugal is wide ventrally. The leading edge of the jugal defines the extent of the maxilla both posteriorly and dorsally. The attachment surface for the jugal constitutes more than half the ascending maxillary process. The contact is rugose along the ventral margin of the attachment area. Anteriorly, the maxilla tapers to a single anterior process. There is a deep groove that originates from the inflexion of the anterior part of the maxilla and continues anteriorly to about half-way between the inflexion point and the tip of the anterior process where it disappears onto the anterior surface. The anterior surface of the maxilla is broad and smooth and is the surface that contacts the premaxilla that lies immediately above. Three prominent foramina are clustered together immediately in front of another larger foramen.

Lingually, there is some damage to the anterior projection of the maxilla. The lingual side of the dental battery is covered by a smooth sheet of bone that appears to be thicker than its mandibular counterpart. The row of mental foramina is highly arched. The ascending process of the maxilla is concave.

The teeth are not as well preserved as those of the dentary. One to two teeth per vertical row participate in the occlusal surface of the maxilla. The central carinae are prominent, but are largely obscured by remnants of the former teeth. No accessory ridges, like those seen on the dentary teeth, are visible.

**Jugal**-- Laterally, the jugal is smooth (Fig. 14C, D). It is, in part, distinguished by a strong, semi-lunate articular surface for articulation

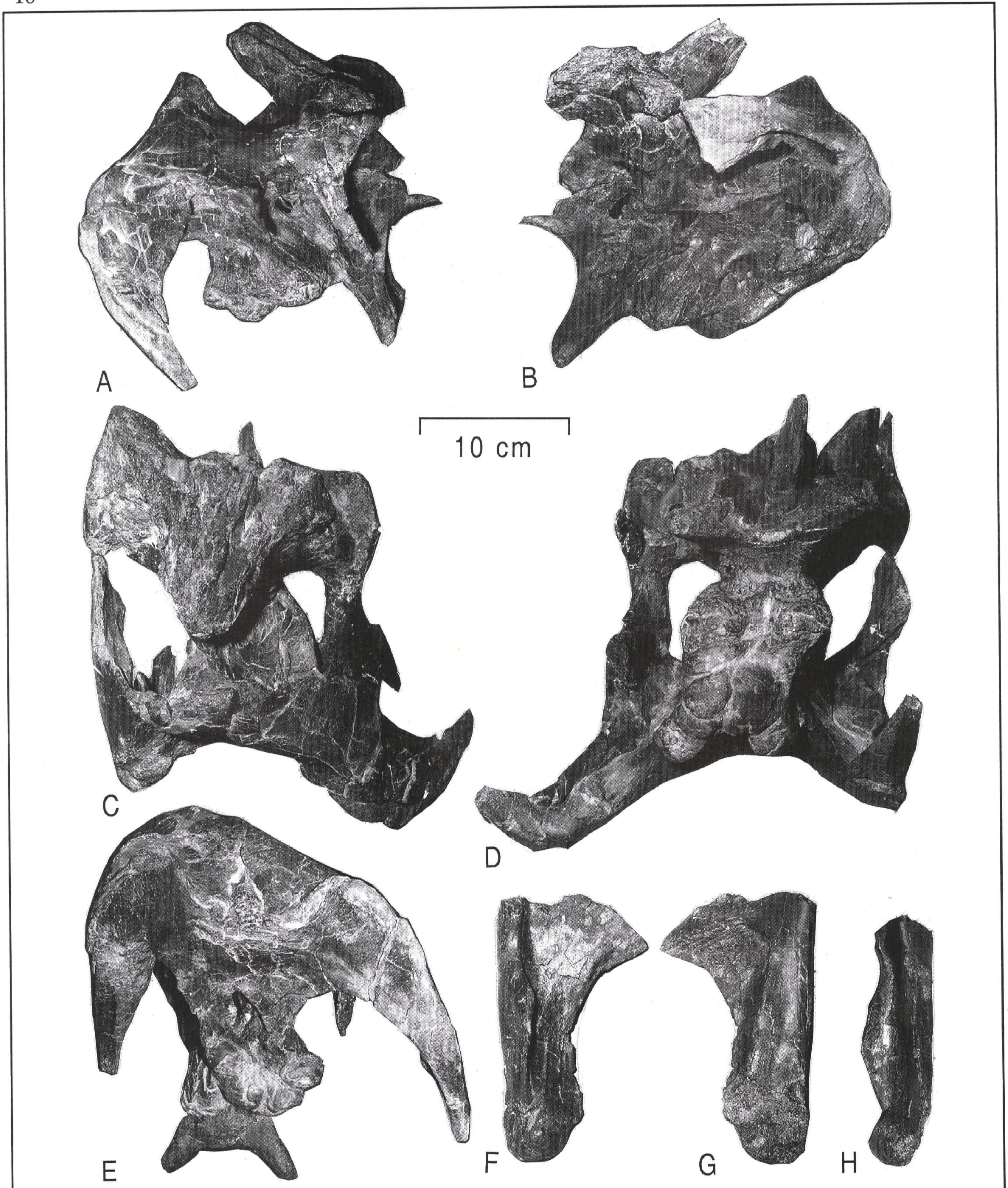


**Figure 8**. *Parasaurolophus tubicen* (PMU.R1250, holotype). Posterior skull region showing (A) right lateral, (B) left lateral view, (C) dorsal, (D) ventral and (E) posterior views. F-H show ventral portion of right quadrate in (F) anterior, (G) medial, and (H) posterior views.

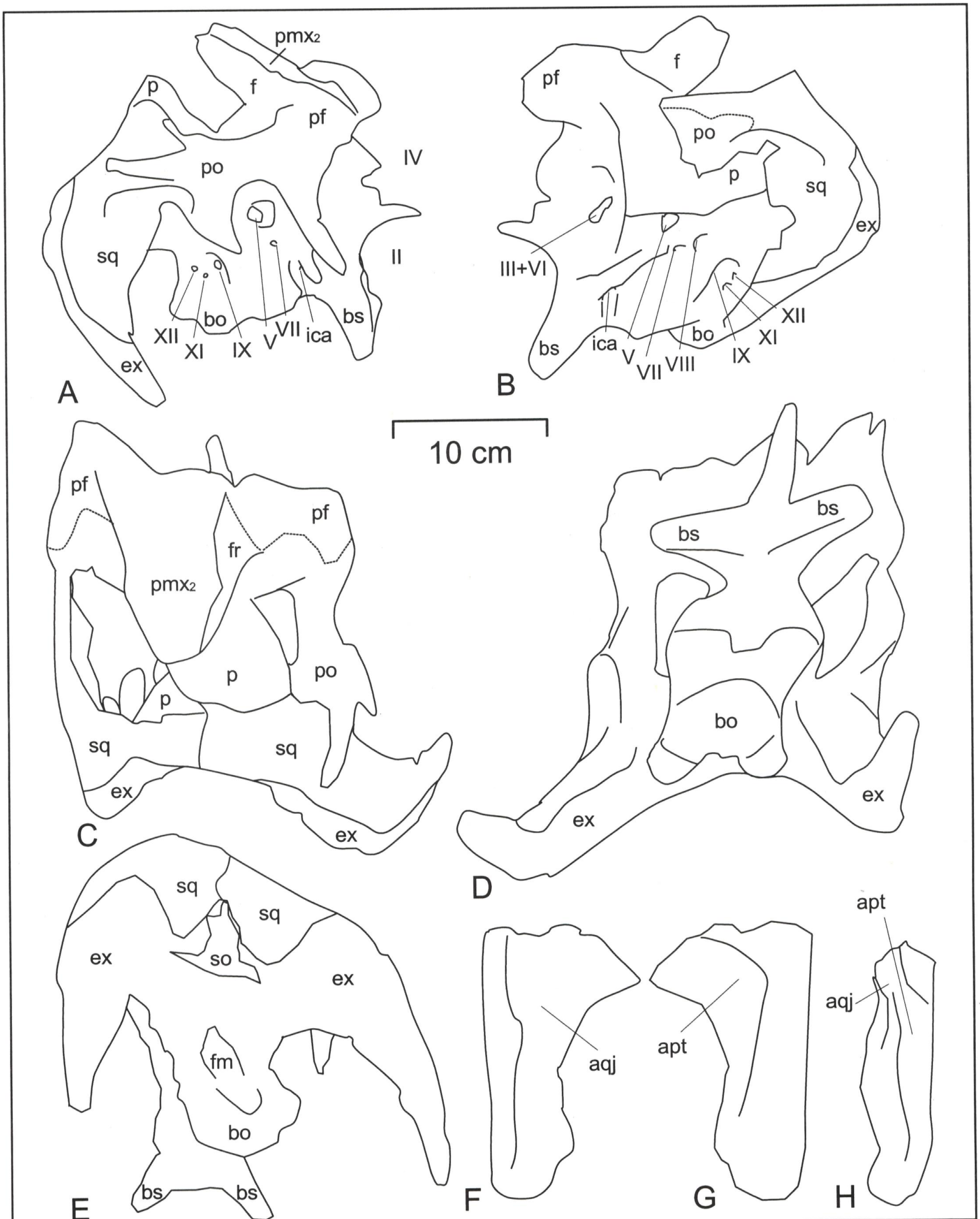


**Figure 9.** *Parasaurolophus tubicen* (PMU.R1250, holotype). Interpretive line drawings showing sutures and osteological features of the posterior skull region in (A) right lateral, (B) left lateral view, (C) dorsal, (D) ventral and (E) posterior views. F-H show ventral portion of right quadrate in (F) anterior, (G) medial, and (H) posterior views. See Appendix 1 for osteological abbreviations. Roman numerals refer to the foramina for the corresponding cranial nerves.

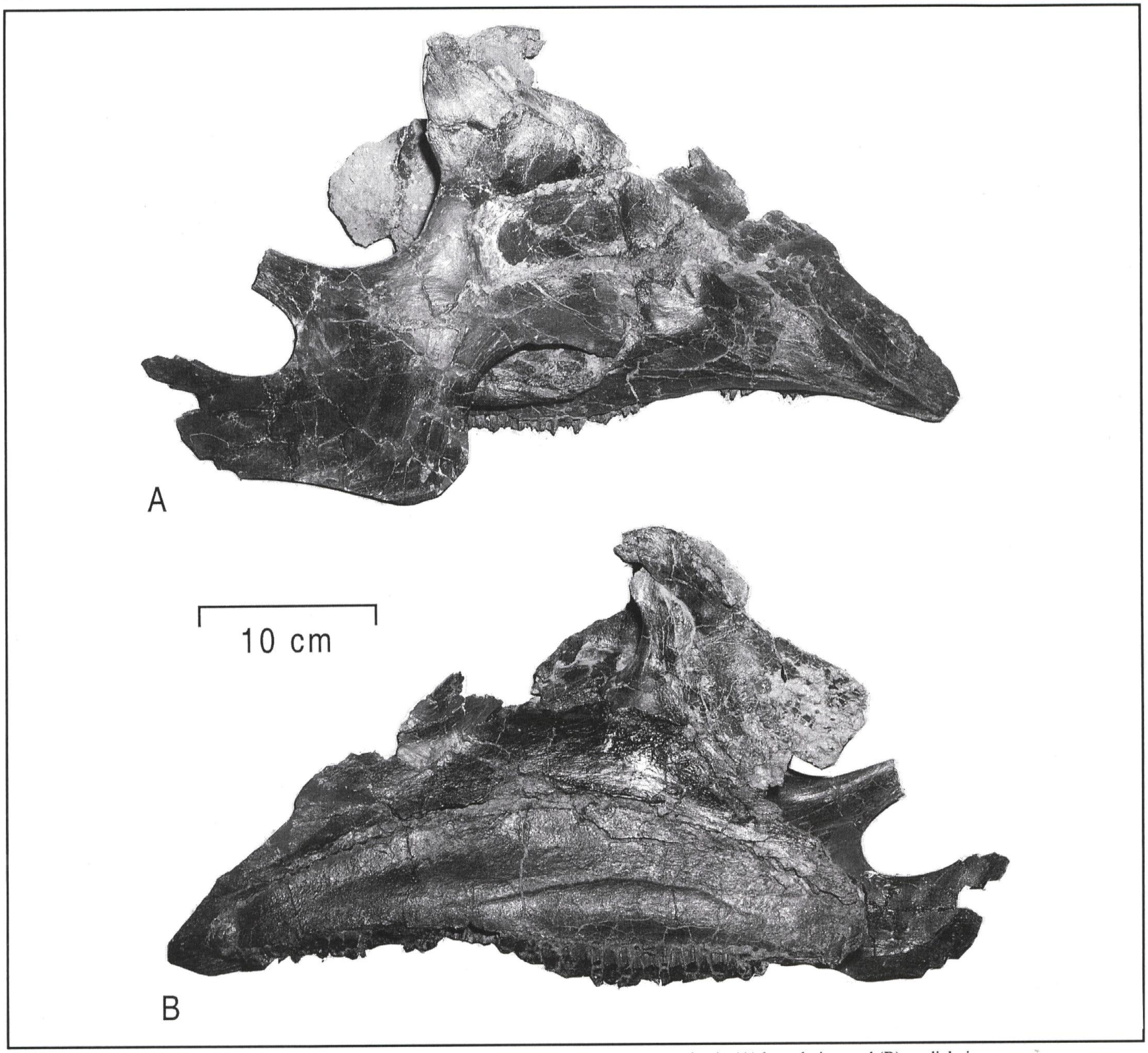


**Figure 10**. *Parasaurolophus tubicen* (PMU.R1250, holotype). Bones of the right maxillary complex in (A) lateral view and (B) medial view.

with the maxilla. The jugal has a strongly curved ventral border and is constricted near its middle. Posteriorly, it has an expanded ventroposterior blade, the upper part of which articulates with the quadratojugal medially. The lower part, near the apex, is marked by a distinct shallow depression. The anterior dorsal border, located anterior to the orbital border, bears a well-developed facet for the reception of the lacrimal. The temporal process rises high to articulate with the descending process of the postorbital; anteriorly, this process is somewhat compressed for the upper half. The medial surface reveals a broad articular surface for the maxilla and pterygoid along the anterior projection of the jugal. The ventral part of the jugal/maxilla contact is characterized by a series of shallow striations. The striations are largely confined to the posterior edge.

**Quadratojugal--** Not recovered.

**Lacrimal--** The lacrimal is sub-rectangular in lateral view (Figs. 16B, 17B) and bears a distinct notch anteroventrally. Laterally, there is a ridge of bone that may represent a line of fusion of the palpebrals (supraoccipitals) to the lacrimal; however, numerous fractures in the basal region make this uncertain. The lacrimal is distinguished by a large, oval, posteriorly directed foramen (lacrimal foramen) situated within the anteroventral region of the orbit. The lacrimal foramen measures 20 mm (maximum dimension). Posteriorly, the lacrimal wedges between the prefrontal and the co-ossified palpebrals. The suture between lacrimal and premaxilla is not evident (due to matrix in this region); however, it is clear that the lacrimal abuts the premaxilla along its entire dorsal margin.

**Prefrontal--** The prefrontal is a prominent bone that rises anteriorly within the orbit between the prefrontal/palpebrals and postorbital and ascends posteriorly to beyond the frontal/nasal contact (Figs. 16B, 17B). Within the orbit, there is an irregular, anteroposteriorly directed offset that looks somewhat like a suture, but that we believe to be a fracture due to post-mortem damage. Dorsally, the prefrontal contacts the premaxilla$_2$ for its entire length, with its posterior portion lapping onto the

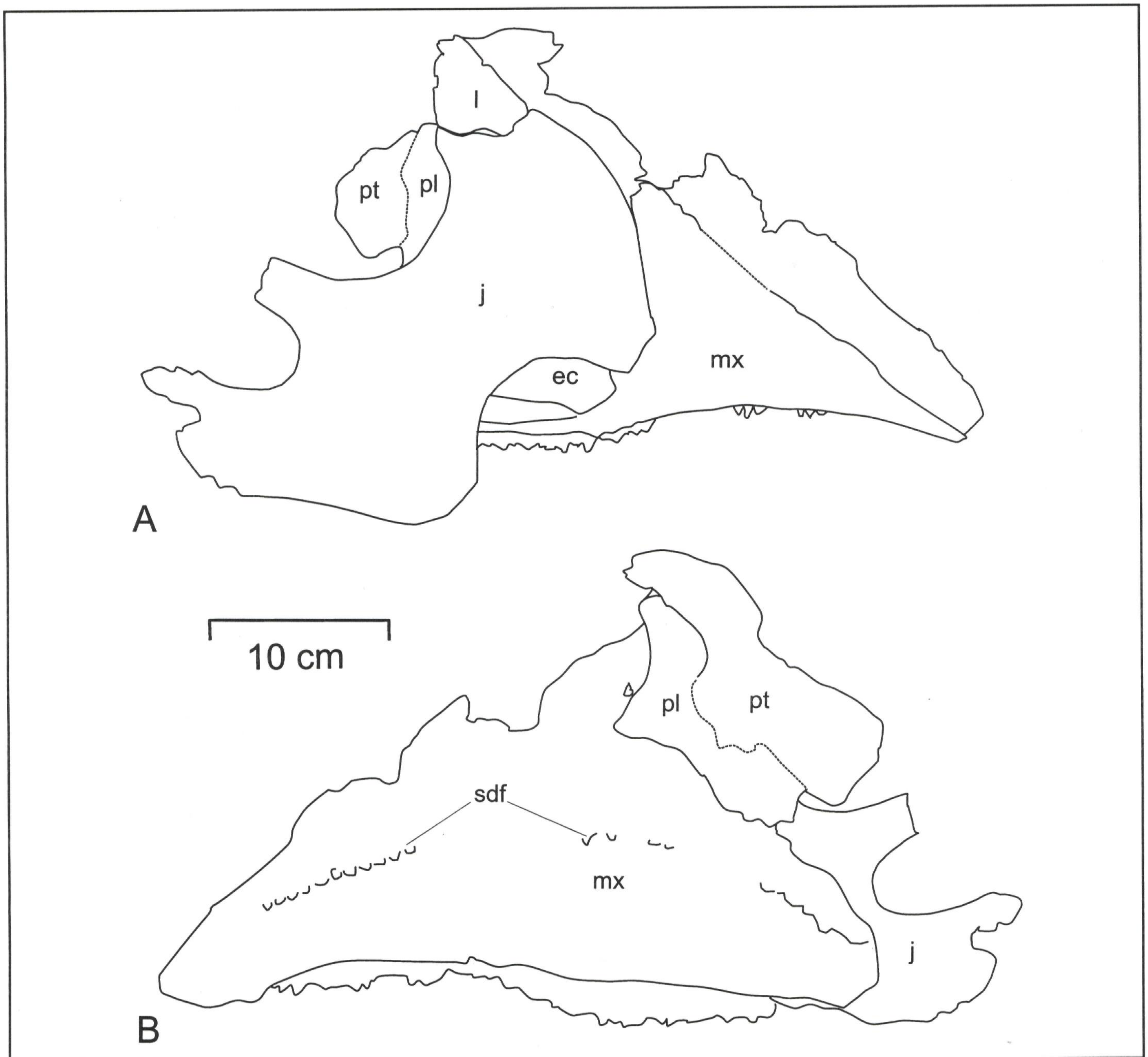


**Figure 11.** *Parasaurolophus tubicen* (PMU.R1250, holotype). Interpretive line drawing showing sutures between the bones of the right maxillary complex in (A) lateral and (B) medial views. See Appendix 1 for osteological abbreviations.

premaxilla$_1$. A medium-sized (15 mm) foramen lies laterally, directly behind the posterior margin of the postorbital/postfrontal contact.

**Frontal**-- Behind the cranial region, in lateral view, the frontals lie with the narial crest just anterior to the nasals (Figs. 16B, 17B) and measure approximately 56 mm from the parietal to the nasals along the midline of the crest. The frontals bulge out laterally and are separated from each other by a distinct suture along the ventral midline of the crest. They strongly interdigitate with the nasals posteriorly and less strongly with the parietal anteroventrally.

Within the posterior region of the orbit, the frontals emerge as slightly rounded bones. Here they are bounded by the prefrontals and postorbital dorsally and the orbitosphenoid ventrally.

**Nasal**-- The paired nasals are confined to the ventral region of the crest, lying immediately behind the frontals (Figs. 16B, 17B). There is a straight suture along the ventral margin of the narial crest that divides these paired elements. They extend subparallel to the crest for a little more than half their length where they then taper to a point posteriorly along the midline of the crest. Their total length is approximately 150 mm. The nasals reach their greatest width at the frontal/nasal contact, which is strongly interdigitate.

**Parietal**-- In lateral aspect, the anterodorsal surface of the parietals is visible; in ventral aspect, the midline is also visible. The parietals extend posteriorly for approximately 95 mm along the midline (sagittal section). They form the medial borders of the supratemporal fenestrae in conjunction with the squamosals, frontals, and postorbitals. The longest dimension of the right supratemporal fenestra is 120 mm; the shortest dimension is 38 mm. The frontoparietal contact is marked by a distinct labyrinthine (complex) suture.

**Postorbital**-- The postorbital articulates with the prefrontal


**Figure 12**. *Parasaurolophus tubicen* (NMMNH P-25100). Right lateral view of nearly complete narial crest, skull roof and basicranium.

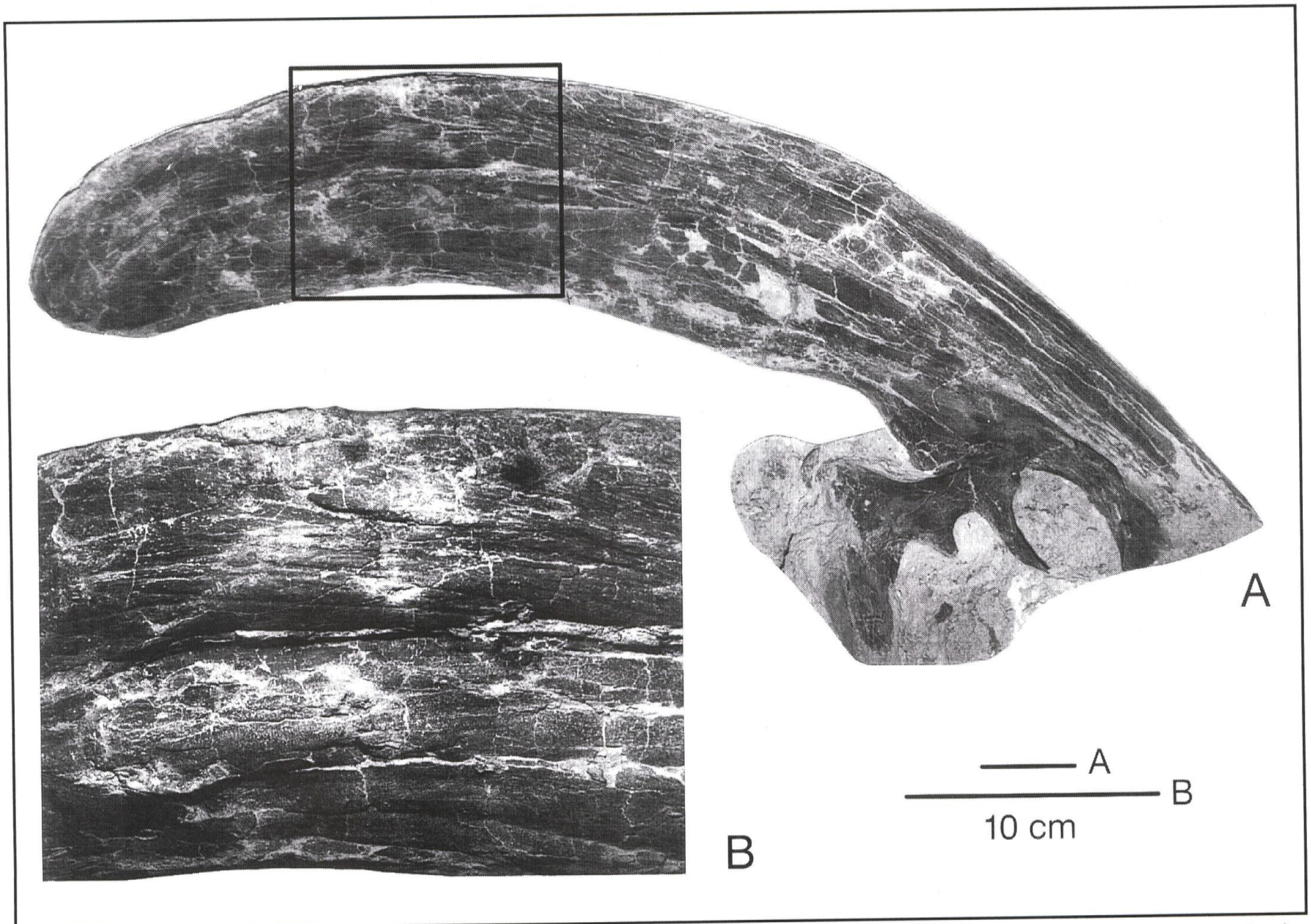


**Figure 13**. *Parasaurolophus tubicen* (NMMNH P-25100). Right lateral view of nearly complete narial crest showing (A) location of (B) close-up, showing anastomosing furrows.

anteriorly, and medially where it joins the prefrontal with a thickened, rugose contact (Figs. 16B, 17B). A small foramen is situated adjacent to the posterior orbital border. Internally, the postorbital appears to articulate with the frontal and the laterosphenoid. Posteroventrally, the postorbital process bears a deep groove for the reception and articulation of the ascending orbital process of the jugal. A concavity, the "postorbital pouch" of Ostrom (1961a), is formed internally above the frontal/postorbital contact and the posterior margin of the orbit. A lesser concavity is situated anterodorsally, within the posterior orbital wall.

**Squamosal**-- The squamosal is a stout element that articulates with the postorbital anteriorly, forming a distinct sigmoidal suture (Figs. 16-17). Anteriorly, the ventral tip of the temporal process of the squamosal, which formed the anterior border of the quadrate, is broken. On the lateral side, there is a single round foramen in the center of the squamosal that measures 4 mm in diameter. The squamosal is further distinguished by a distinct posterodorsally directed process, directed posteromedially toward the parietal.

**Quadrate**-- Not recovered.

**Palatal Elements**

**Vomer**-- Not recovered.

**Palatine**-- On the lingual surface of the palatine, the posteroventral flange is free and not attached to the maxilla (Figs. 14A, B, 15). The posterior edge of the palatine bears an attachment for the overlapping sutural contact of the pterygoid (overlapping the lingual side). The dorsal surface of the palatine is distinguished by a poorly preserved rugose process. Anteriorly, the antorbital fenestra is divided by extensions of the maxilla and palatine that join each other.

Laterally, the palatine articulates with the maxilla and jugal. The palatine/jugal contact is situated behind the ascending maxillary process and is characterized by a very rough or rugose surface.

Due to distortion along the lower region of the maxilla, the contact between the palatine and ectopterygoid cannot be distinguished. The antorbital fenestra is a single opening that emerges posteriorly between the lateral inner side of the maxilla and the labial surface of the palatine.

**Pterygoid**-- Not recovered.

**Ectopterygoid**-- The ectopterygoid lies above the posterior maxillary shelf. It is a thin, sheet-like bone posteriorly overlapping the posterior-most margin of the maxilla. The posterior edge is rugose where it contacts both the palatine and pterygoid.

**Basicranial Elements**

The basicranium (Figs. 16-17) consists of the basioccipital, basisphenoid, laterosphenoid, presphenoid, orbitosphenoid, prootic and opisthotic. The arrangement of foramina of the cranial nerves is similar to the arrangement reported for *Corythosaurus* by Ostrom (1961a). Moreover, the region of the foramen for the trigeminal nerve (V) is nearly identical to *Corythosaurus*, with a well defined groove for the ramus profundus ($V_1$) and channel for the ramus mandibularis ($V_3$). The channel for the ramus maxillaris ($V_2$) of the trigeminal nerve is shallow and not well defined. The maximum diameter of the foramen for the trigeminal nerve opening is 15 mm, half the size of that reported for *Corythosaurus* (Ostrom, 1961a). There is a distinct suture between the laterosphenoid and the prootic.

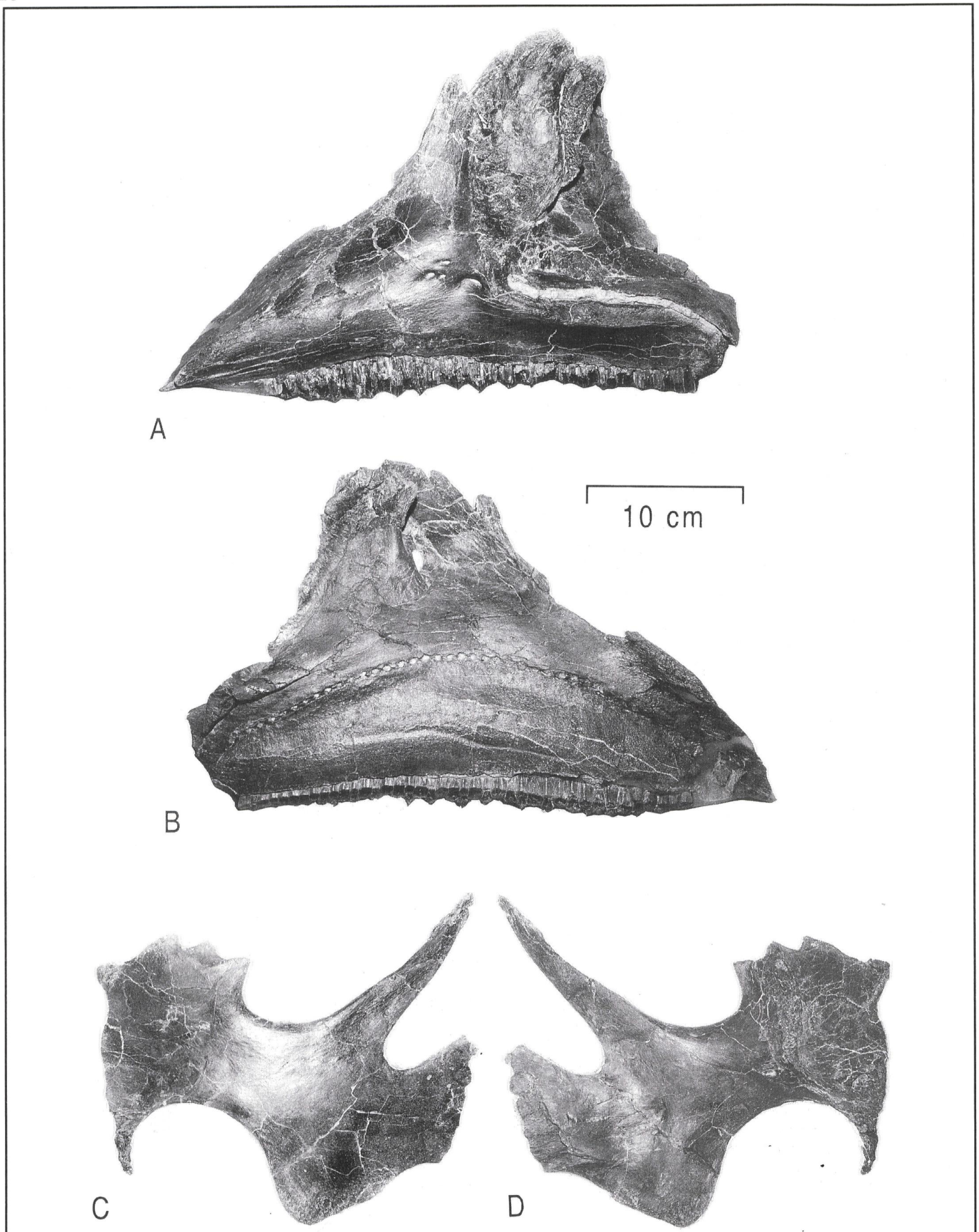


**Figure 14**. *Parasaurolophus tubicen* (NMMNH P-25100). Bones of the left maxillary complex in (A) lateral and (B) medial views. Left jugal in (C) lateral and (D) medial views.

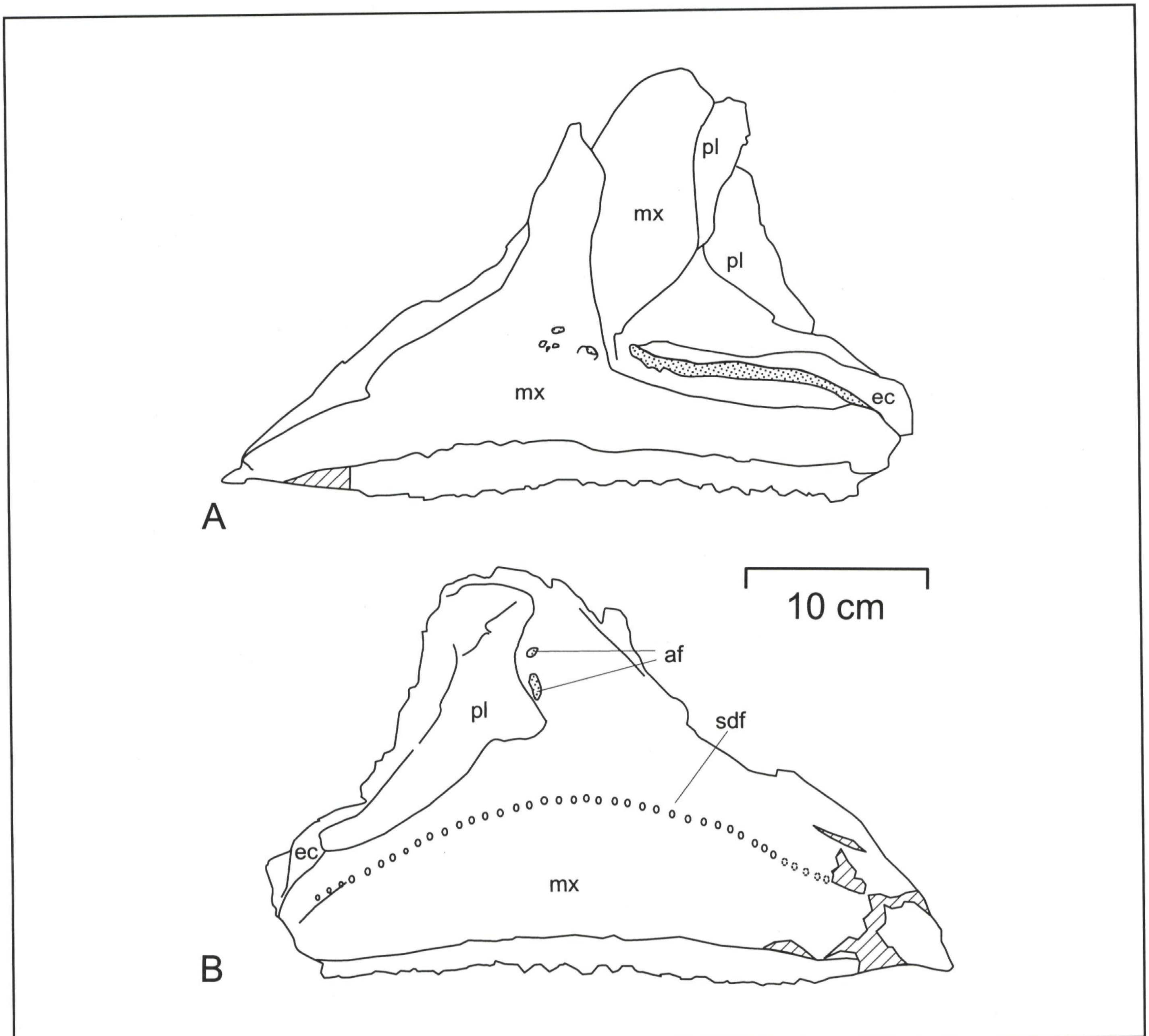


**Figure 15**. *Parasaurolophus tubicen* (NMMNH P-25100). Interpretive line drawings of a portion of the left maxillary complex (A) lateral and (B) medial views. See Appendix 1 for osteological abbreviations.

**Supraoccipital**-- The supraoccipital (Figs. 16A, 17A) is poorly preserved and highly distorted due to crushing. It is wedged between the exoccipital below and the squamosals dorsolaterally.

**Exoccipital-Opisthotic Complex**-- In posterior view (Figs. 16A, 17A), the exoccipital is incomplete and only the right exoccipital is completely intact. It is a distinctive bone, not unlike those seen in other hadrosaurs. It contacts the squamosal dorsolaterally, forming the paroccipital process. The lateral surface of the exoccipital portion of the paroccipital process has a rugose texture for its entire length. The paroccipital descends to a point. Dorsolaterally, the exoccipital-opisthotic complex is bordered by the squamosal for its entirety. In posterior view, the exoccipital contacts the supraoccipital region. Anteriorly, the exoccipital-opisthotic complex contacts the prootic.

**Basioccipital**-- In posterior aspect, the occipital condyle (Figs. 16A, 17A) has a spongy, rugose texture and is partly crushed, especially on the left side. Above the basioccipital portion of the condyle lies the foramen magnum, which is also distorted laterally. In right lateral view, the basioccipital joins the exoccipital-opisthotic complex dorsoposteriorly, the prootic dorsally, and the basisphenoid anteriorly. The sutures separating these bones are partially obscured. The suture between the basioccipital and the exoccipital/opisthotic complex is not evident. That between the basisphenoid and the basioccipital is distinct and is oriented near vertical and divides the basisphenoid/basioccipital tubercles.

Dorsally, foramina for cranial nerves IX, X, XI, and XII are present and lie along the base of the exoccipital/opisthotic complex (Fig. 17B). The division between these regions is not completely discernible. However, there is a short (10 mm) posterior suture segment that extends from cranial nerve foramina IX, X, and the jugular foramen, in a sigmoidal pattern. Cranial nerve foramen XII is smaller (2.5 mm) than foramina for cranial nerves IX and X and the jugular foramen (all 4 mm in diameter) and lies anterior to the sigmoidal suture. The foramen for cranial nerve XII is approximately the same size (5 mm) in diameter. The

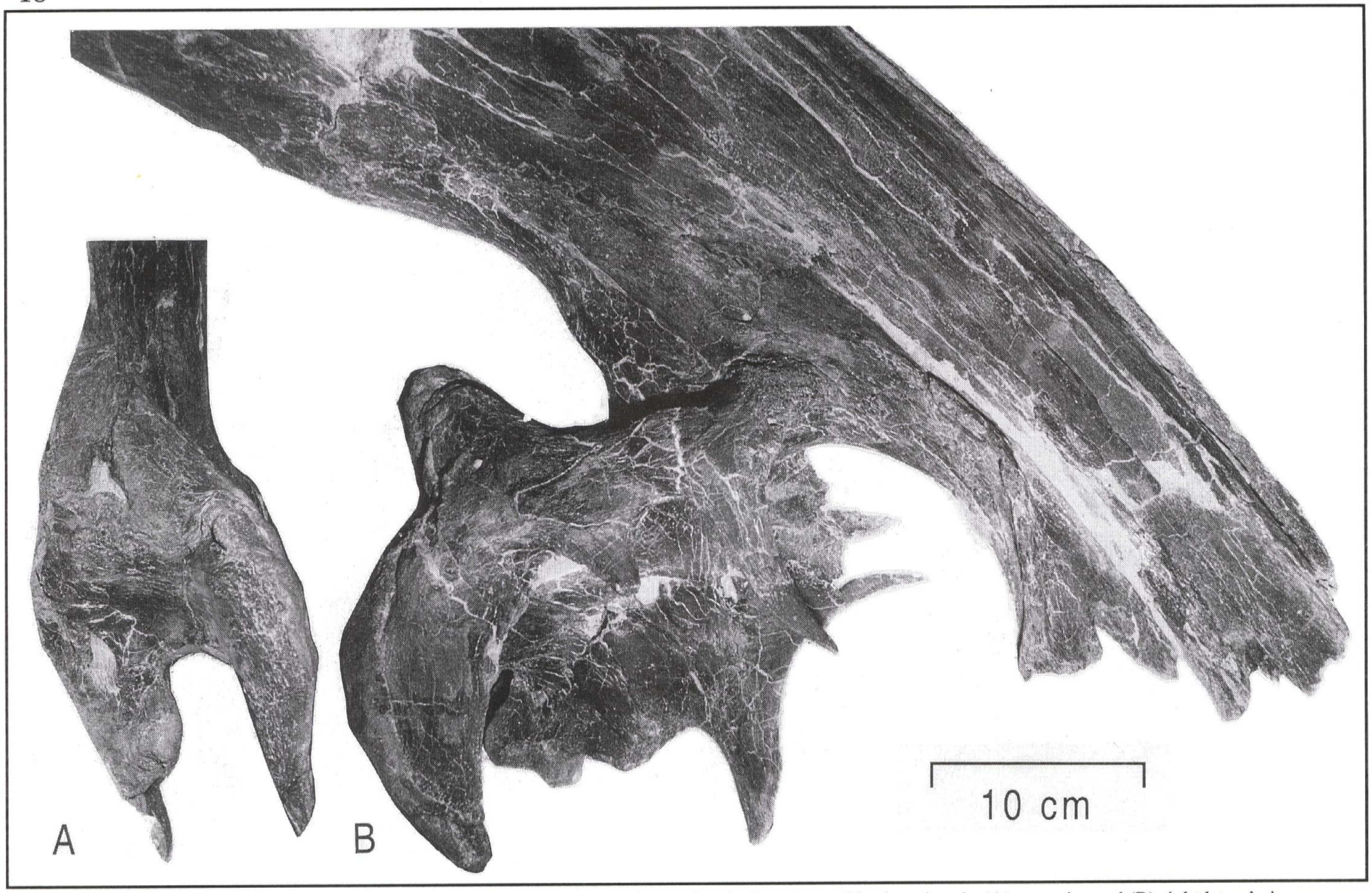


**Figure 16**. *Parasaurolophus tubicen* (NMMNH P-25100). Close-up view of posterior skull region and basicranium in (A) posterior and (B) right lateral views.

foramen for cranial nerve VIII is located at the juncture of the basioccipital, prootic, exoccipital/opisthotic complex and basisphenoid. This foramen measures approximately 20 mm in diameter (maximum), making it sub-equal to that of the foramen for cranial nerve V. Deep within the passage of cranial nerve VIII is a delicate horizontal septum, which is oriented anteroposteriorly and divides it into two sub-equal parts. The upper part is the fenestra ovalis and the lower the fenestra pseudorotunda (Ostrom, 1961a).

**Prootic**-- The prootic is a relatively large, irregularly shaped bone that is bordered posteriorly by the exoccipital/opisthotic complex and basioccipital, anteriorly by the laterosphenoid, anteroventrally by the basisphenoid and dorsally by the parietal (Figs. 16-17). The contact with the parietal is on the lateral roof of the braincase (at present obscured by matrix).

The sutures delineating this bone from the lower elements (i.e., basioccipital, basisphenoid and the lower part of the laterosphenoid, below the foramen for cranial nerve for V) are not visible (see Fig. 17B). Dorsally, a suture clearly marks the prootic/laterosphenoid contact, which extends dorsally from the foramen for cranial nerve V up to the lateral side of the braincase. The suture that separates the prootic from the exoccipital/opisthotic complex arises from the foramen for cranial nerve VIII and extends dorsally to the lateral side of the braincase. In lateral view, there are a series of fractures running between the two foramina and an abrupt lateral displacement of the bone. The foramen for cranial nerve VII opens ventrally, below the fracture (displacement). There is a prominent ridge, or flange, that extends from below the foramen for cranial nerve V. Ventrally, it terminates in a small flange that forms the posterior border and the lower-most extent of the prootic, behind which lies the posterior part of the basisphenoid. Behind this flange abuts another ridge that extends ventrally beyond the lower part of the prootic and becomes part of the lateral border of the basisphenoid.

The anterior margin of the prootic is distinguished by an irregular raised ridge that extends from the ventral flange up to the ventral margin of the foramen for cranial nerve VI. The basisphenoid lies anterior to this margin. Anterodorsally, the contact between the posteroventral part of the laterosphenoid and the anterodorsal edge of the prootic lies within the groove of the profundus ramus of the trigeminal nerve. A groove for the third trigeminal branch (ramus mandibularis) extends ventrally from the foramen for cranial nerve V.

**Basisphenoid (includes the parasphenoid)**-- Only the right lateral side of this complex region is visible (Figs. 16B, 17B). The basisphenoid contacts the basioccipital posteriorly and is overlapped laterally by the prootic. Anterodorsally, the basisphenoid contacts the orbitosphenoid and the presphenoid. The channel for the internal carotid artery lies immediately behind the flange that defines the lower limit of the prootic.

The right pterygoid process of the basisphenoid is 70 mm long from the posterior base to the distal tip. The anterior margin of the basisphenoid forms an arc that measures 190 mm to the distal tip of the parasphenoid process. The foramen for the internal carotid artery lies anterior to the basal tuber, at the apex of a deep groove that exits lateroventrally. The surface of the basisphenoid is relatively smooth and concave adjacent to the anterior margin.

The parasphenoid forms an anteriorly directed process that is continuous with the basisphenoid. A vertical break at the base of this process may mark the sutural contact between the parasphenoid and the basisphenoid.

**Orbitosphenoid-Presphenoid Complex**-- The orbitosphenoid and

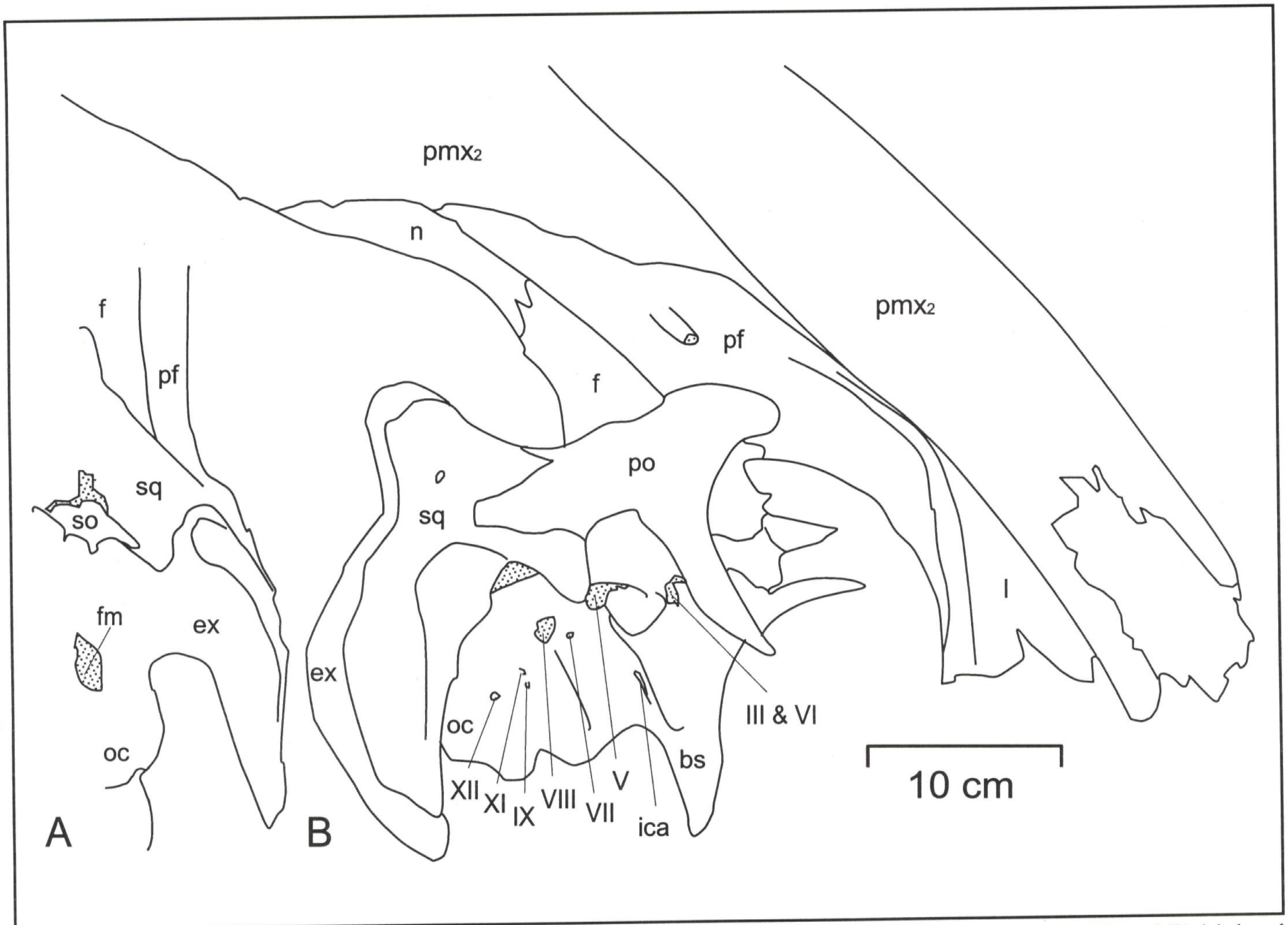


**Figure 17**. *Parasaurolophus tubicen* (NMMNH P-25100). Interpretive line drawings of posterior skull region and basicranium in (A) posterior and (B) right lateral views. See Appendix 1 for osteological abbreviations. Roman numerals refer to the foramina of the corresponding cranial nerves.

presphenoid form part of the posteromedial wall of the orbit. This region is relatively smooth, and the two elements form a mostly concave surface. They are bounded ventrally by the basisphenoid, posteriorly by the laterosphenoid, and dorsally by ty the frontal.

At the juncture of the orbitosphenoid, laterosphenoid and basisphenoid lies the foramen for cranial nerve III (Fig. 17B). On the orbitosphenoid portion of the complex, there is a small foramen that we interpret as the exit for cranial nerve IV, lying approximately 10 mm above the foramen for cranial nerve III. Anterior to the foramen for cranial nerve III there is a foramen for cranial nerve II.

There appears to be a suture between the foramina for cranial nerves III and II, which marks the separation of the presphenoid (below) and the orbitosphenoid (above). This suture is not distinct anteriorly. Extending forward from the foramen for cranial nerve III is an irregular suture that is oriented horizontally, extending anteriorly to the base of the parasphenoid process, which divides the presphenoid from the basisphenoid.

**Laterosphenoid**-- The laterosphenoid is sub-triangular in lateral view and is bounded posteroventrally and ventrally by the prootic, dorsoposteriorly by the parietal, anteriorly by the orbitosphenoid, dorsally by the frontal, and dorsolaterally by the postorbital. The dorsoposterior extent of the laterosphenoid participates in the anteromedial portion of the supratemporal fenestra. The foramen for cranial nerve V is at the posterior ventral corner of the laterosphenoid. Apparently, the ventral contact with the prootic occurs within the channel for the profundus ramus of the trigeminal nerve. No suture can be detected anteriorly between the laterosphenoid and the orbitosphenoid.

**Mandibular Elements**

**Predentary**-- Not recovered.

**Dentary (including the dental battery)**-- The nearly complete left dentary (Fig. 18) and tooth battery (Fig. 19) (see Appendix 2 for measurements) are well preserved. Six mental foramina are located midway between the ventral surface and the ventral margin of the tooth row (anteriorly) concentrated towards the front. Except for numerous "micro" fractures, the element is in excellent condition. Laterally, the dentary is smooth, the ventral surface is concave, bowing anteroventrally. The large coronoid process has a broad base and ascends slightly anteriorly. The coronoid is constricted approximately two-thirds above its base, where it is distinguished by a convex anterior edge that becomes straight posteriorly. The dorsoposterior corner of the coronoid process is squared-off. The surface of the coronoid shows scarring on the inner (medial) side. The anterior, or leading edge of the coronoid, is thickened and slightly rugose. The posterior surface narrows to a blade-like edge. Posteromedially, there is a large cavity behind (medial to) the cornoid.

The dental battery (Figs. 18-19) is nearly complete. The lingual side is, in part, covered by a sheet of bone, which conceals the replacement teeth. It is slightly depressed, cracked and covered by numerous small fractures. As many as three teeth per vertical row are visible where this sheet of bone is damaged. More than 40 "special" (nutrient) dental

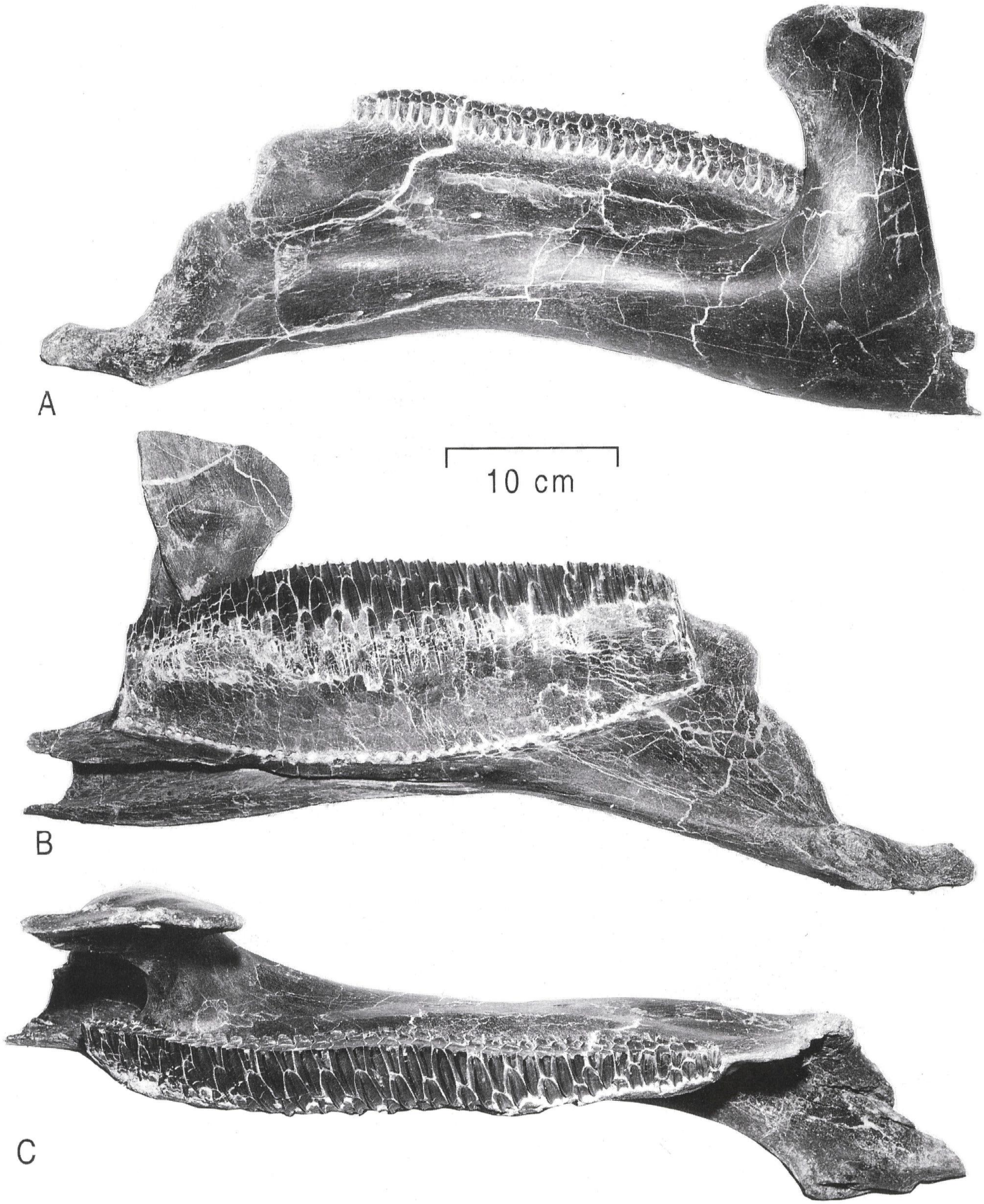


**Figure 18**. *Parasaurolophus tubicen* (NMMNH P-25100). Left dentary in (A) lateral, (B) medial, and (C) dorsal views.

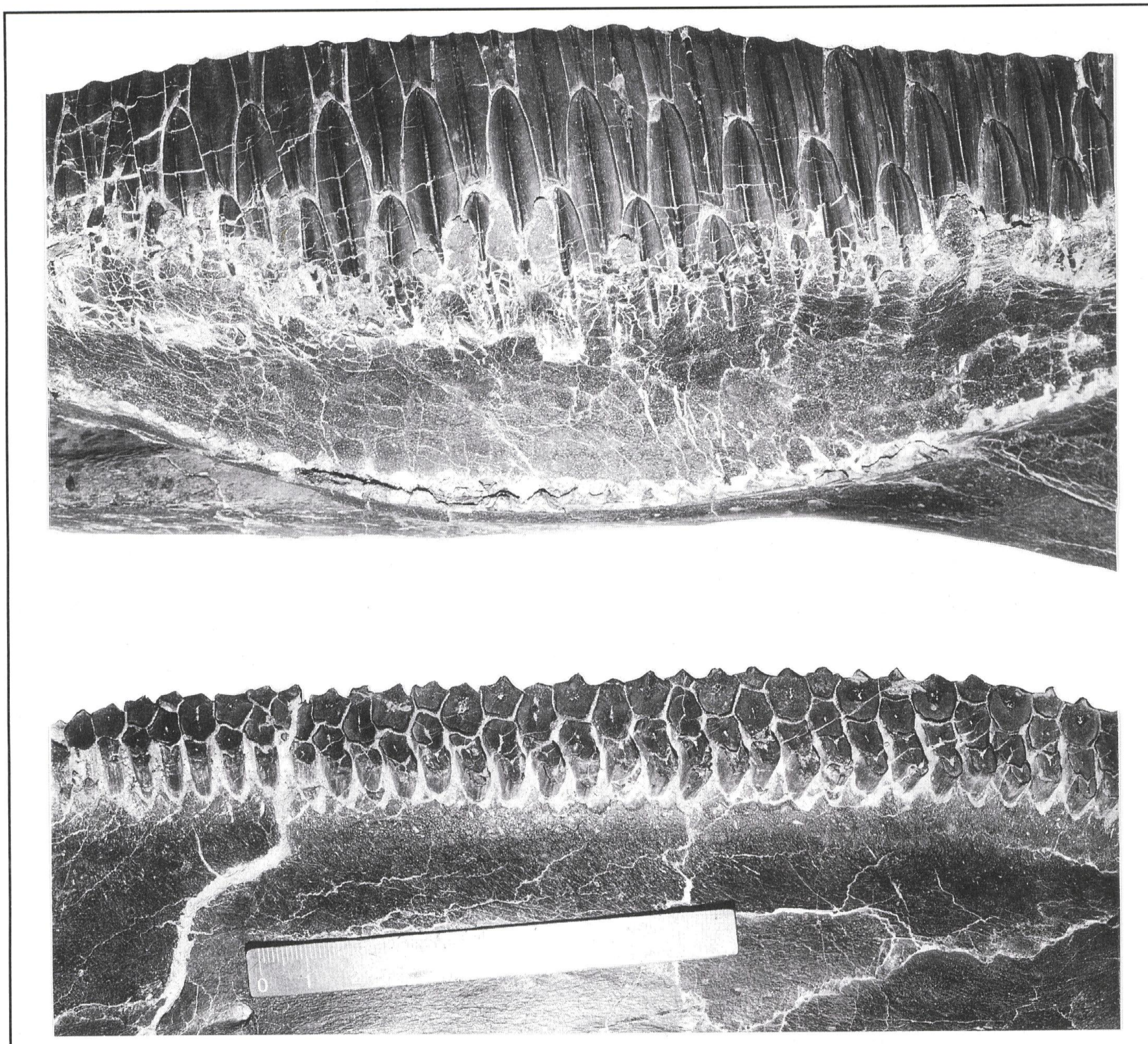

**Figure 19**. *Parasaurolophus tubicen* (NMMNH P-25100). Close-up of dentary teeth in (upper) lingual, and (lower) labial views. Note that scale bar = 10 cm.

foramina are visible along the base of the dental battery.

Anteriorly, the short dental shelf drops off sharply and forms a sinuous anterior contact for the attachment for the predentary. The symphysis of the dentary is long, smooth, and marked by a distinct median groove. The groove originates from the posterior margin and tends ventrally half way along the symphysis. The teeth of the dentary (Fig. 19) are elongate and are distinguished by a central, slightly sinuous carina. The sinuous nature is especially visible on the anterior teeth. Minute denticles are present on the anterior teeth along the anterior and posterior edges of the tooth. Faint parallel ridges are present on some teeth between the carina and anterior cutting edges. The occlusal surface has as many as four teeth (towards the mid-point) per vertical row which participate in the formation of the grinding surface. The dental replacement pattern corresponds to the "abnormal pattern" noted by Ostrom (1961a), where, from anterior to posterior, the teeth ascend to the mid-point of the dental battery (relative to the occlusal surface) at which point they remain subparallel to the occlusal surface. The shape of the occlusal surface is sinuous and is opposite that of the maxillary occlusal surface.

**Surangular**-- The articular region of the surangular (Fig. 20A-D) is angled laterally. The surangular articulates with the dentary anteriorly. A strong lateral ascending process laps onto the posterior margin of the coronoid process. This process is displaced medially and represents a post-mortem break. The "floor" of the surangular, which lies posteriorly,is a continuation of the Meckelian fossa of the dentary. This fossa is ringed by muscle scars along the dorsal margins of the walls of the fossa. A distinctive flange of bone rises from the posterior end of the medial surface, which articulates to the splenial. A large, pitted protuberance is situated anterolaterally in front of the condylar facet. This distinctive region probably served as part of the insertion of the M. adductor mandibulae externus. A prominent foramen pierces the dorsolateral region of this protuberance. The entire region is highly pitted and rugose and departs from other hadrosaurid surangulars in this respect (Ostrom, 1961a). Ventrally, the surangular is smooth and

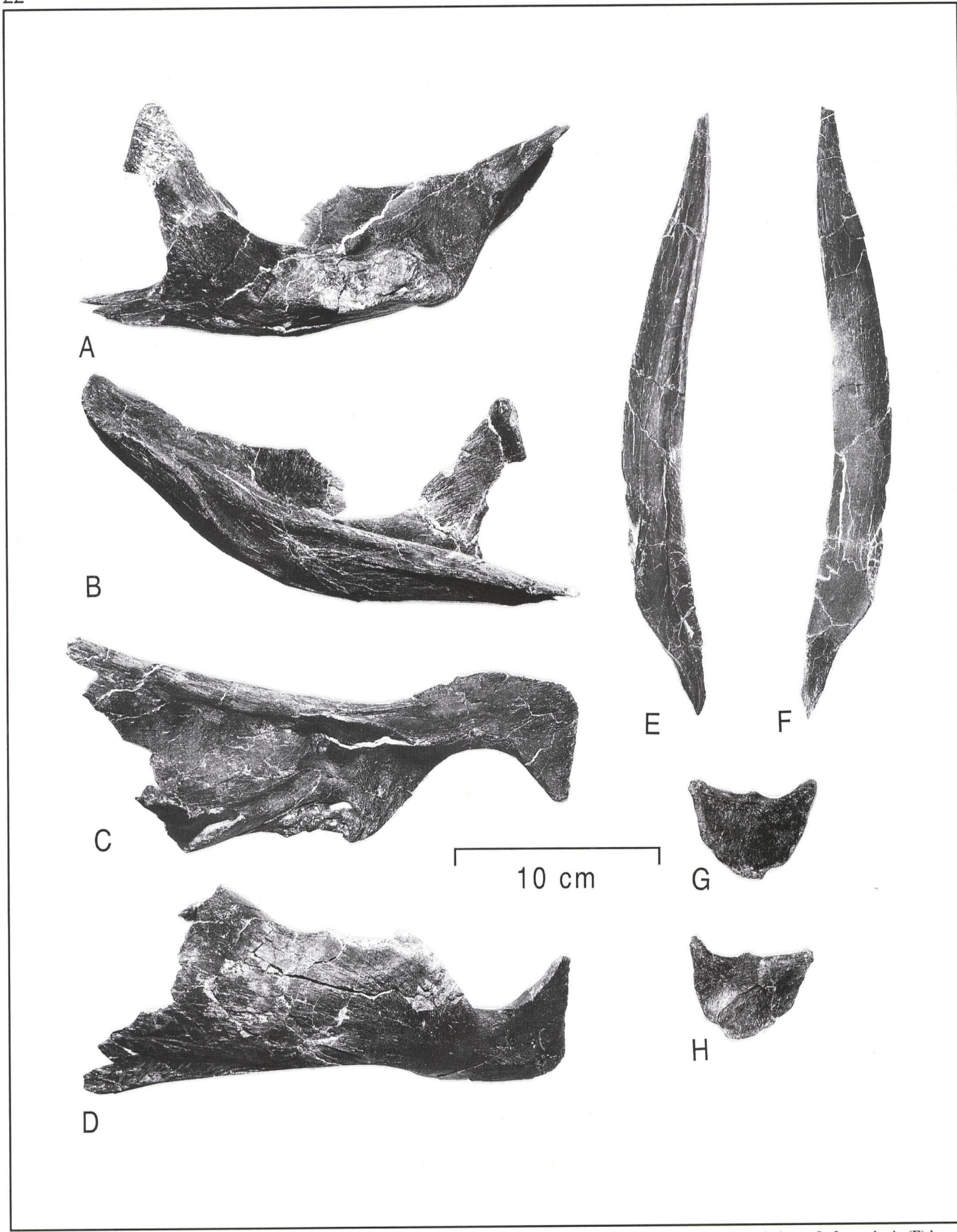


**Figure 20**. *Parasaurolophus tubicen* (NMMNH P-25100). Left surangular in (A) lateral, (B) medial, (C) dorsal, and (D) ventral views. Left angular in (E) lateral and (F) medial views. Left articular in (G) dorsal and (H) ventral views (anterior end is up).

convex. The anterior attachment surface for the dentary articulation is striated anteroposteriorly.

**Angular**-- The angular (Fig. 20E, F) is a narrow bone measuring 300 mm (maximum length) and 30 mm (maximum depth). It has been slightly distorted as it does not articulate well with the dentary, surangular, and angular. It has a blade-like, elongated, boat-shaped appearance in lateral view. Posteriorly, it rises and tapers to a point. Anteriorly, it ascends slightly, then curves downward. There is a groove along the anterodorsal surface. The groove rises anteriorly and can be traced posteriorly for most of its length. Dorsally, the angular is nearly straight for its entire length, with a slight medial curve for the last 50 mm. Anterodorsally, the internal surface bears a prominent groove that rises 40 mm from the anterior-most tip and extends posteriorly for about 100 mm, where its opens to a broad surface under an articulation facet. Dorsally, the articulation surface for the splenial is directed upward (anteriorly) and is positioned posterolaterally. The ventral border bears a ridge for nearly 75% of its enire length. Posteriorly, a broad articular surface is present for the attachment to the surangular.

**Articular**-- The articular (Fig. 20G, H) is sub-concave in shape. It articulates with the surangular ventrally. The glenoid fossa of the articular is not well defined. The bone is at its thickest at the anterior end, and it tapers to a thin edge medially and posteriorly. Anteromedially, there is a pronounced, deep and somewhat rugose facet for the articulation of the splenial.

**Splenial**-- not recovered.

**Discussion--** NMMNH P-25100 is remarkably similar to the holotype of *P. tubicen*, in that it shares a number of apomorphic features so that we are certain of its taxonomic assignment. Moreover, the preservation of the new specimen is nearly identical to that of *P. tubicen*, suggesting that Sternberg collected the holotype from the same stratigraphic interval (i.e., the De-na-zin Member of the Kirtland Formation, see discussion below).

## INTERNAL MORPHOLOGY OF THE NARIAL CREST (based on computerized tomography)

Based on examination of natural breaks, cut sections, or "dissection" of the crests in the few existing specimens previous workers have interpreted the internal structure of the narial crest of *Parasaurolophus* as a relatively simple arrangement of tubular passages.

Parks (1922) was the first to illustrate a narial crest in cross-section, based on a break in the crest of ROM 768 (*P. walkeri*). The break revealed two pairs of tubes, two dorsal and two ventral, with the right and left sides separated by a medial (sagittal) septum.

In his publication describing the holotype of *P. tubicen*, Wiman (1931) also illustrated a break in the narial crest. This cross-section is much compressed laterally (our personal observation), making interpretation of the tubal passageways of the narial crest difficult. Like Parks (1922), Wiman interpreted the narial cross-section as a rather simple structure, based on a basal break in the narial crest (Wiman, 1931; plate 2, figure 6), with a single dorsal passage above and a ventral passage below. Wiman (1931) showed no septa dividing the narial crest into left and right and dorsal and ventral tubes in his cross-sectional reconstruction.

Weishampel (1981b) studied the narial chambers of *Parasaurolophus* (*P. walkeri* and *P. cyrtocristatus*), and described them as consisting of laterally paired tubes that rise posterodorsally from the external nares, extend to the tip of the crest where they make a U-bend, and return ventrally to terminate in a common median chamber above the skull roof. A short, single passageway descends from the common median chamber to the choana. Additional, laterally paired passageways, the lateral diverticulae, arise from the common median chamber and ascend posterodorsally between the ascending dorsal and ventral tubes to approximately half the length of the crest, forming long, cylindrical cul-de-sacs.

As noted above, the new specimen of *P. tubicen* (NMMNH P-25100) includes a nearly complete narial crest (Fig. 12), lacking only the segment below the lacrimal. The narial crest, as in the type specimens of the long-crested *P. walkeri* and *P. tubicen*, is separated into dorsal and ventral components by a longitudinal groove that extends from the premaxilla/maxilla suture and continues on each side for nearly its entire length. Externally, the dorsal component is marked by numerous anastomosing furrows directed dorsoposteriorly, resulting in a crenullated surface. The external surface of the ventral component of the crest is relatively smooth.

A series of about 350 computerized tomography (CT) slices (cross-sections) and a radiograph using a General Electric high speed helical CT scanner were taken of the skull and crest at 3 mm intervals (see Appendix 3). CT slices of some of these are presented in Appendix 3. The CT data and radiograph show an arrangement of tubes unlike those described previously for *Parasaurolophus* (Fig. 21). The dorsal component of the crest contains three pairs of tubes: a pair of dorsal tubes, a pair of median tubes, and a pair of lateral tubes that flank the median tubes. All the tubes of the dorsal component are present above the lacrimal and presumably originate from the external nares. Each of the dorsal pair of tubes ascends to the tip of the crest where it forms a U-bend, returns inside the ventral margin of the crest for a relatively short distance, and terminates in a large chamber. The dorsal pair of tubes is not a direct conduit between the external nares and the choana. The chambers of the dorsal tubes are apparently separated by a thin median septum. The lateral and medial tubes of the dorsal ascending series roughly correspond to the dorsal ascending tracts of Weishampel (1981a, b) and are considered active tubes. These tubes rise from the external nares and ascend to nearly the tip of the crest where each of the laterally paired set of tubes coalesce into a single tube. These tubes form a U-bend, and return inside the ventral part of the crest as tubes that correspond to the ventral ascending tracts of Weishampel (1981a,b).

The lateral diverticulae are not simple cylindrical tubes, as previously described by Weishampel (1981a, b). Each is composed of a dorsal tube that originates below the skull roof, between the orbits, and extends part way up the crest, forming a tight U-bend and returning as a ventral tube above the ventral ascending tract. The paired ventral tubes of the lateral diverticulae coalesce with the paired ventral ascending tracts near the base of the crest in an area that roughly corresponds to the common median chamber of Weishampel (1981a, b). However, this common chamber is not medial, but is divided by a median septum. The ventral ascending tracts and the dorsal component of the lateral diverticulae presumably lead to a choana within the skull, and consequently are also not part of the direct conduit (from the external nares to the choana).

## *PARASAUROLOPHUS CYRTOCRISTATUS* Ostrom, 1961b
### Figures 1D, E, 22-29

**Holotype**-- FMNH P27393, incomplete narial crest, portions of the skull roof, part of left lower dentary (see below), and incomplete postcranial skeleton (Figs. 1D, 22-25).

**Revised diagnosis**-- *Parasaurolophus cyrtocristatus* differs from both *P. walkeri* and *P. tubicen* in having a short narial crest that curves sharply posteroventrally. Internal network of simple, paired tubes that extend from the external nares posteriorly to the apex of the narial crest where they make a U-bend and continue anteriorly where they descend into the choana of the skull; lateral diverticulae situated medially between the dorsal ascending tracts and ventral ascending tracts and divided dorsally by an internal sagittal septum descending from the floor of the paired dorsal ascending tracts.

**Redescription of the skull**-- This skull, which consists of an incomplete narial crest (premaxillae$_2$), fragmentary skull roof (Figs. 22-23), and a portion of the left lower jaw (Fig. 25), served solely as the basis for the diagnosis of this species (Ostrom, 1961b). However, in a subsequent paper, Ostrom (1963), revised his earlier diagnosis of the